Science Translational Medicine
AAAS

Unimolecular Dual Incretins Maximize Metabolic Benefits in Rodents, Monkeys, and Humans

Brian Finan *et al.*

Sci Transl Med **5**, 209ra151 (2013);
DOI: 10.1126/scitranslmed.3007218

Editor's Summary

"Twincretins": Two Is Better than One

Despite obesity-linked diabetes approaching worldwide epidemic proportions and the growing recognition of it as a global health challenge, safe and effective medicines have remained largely elusive. Pharmacological options targeting multiple obesity and diabetes signaling pathways offer greater therapeutic potential compared to molecules targeting a single pathway. Finan *et al*. now report the discovery, characterization, and translational efficacy of a single molecule that acts equally on the receptors for the incretin hormones glucagon-like peptide-1 (GLP-1) and glucose-dependent insulinotropic polypeptide (GIP). In rodent models of obesity and diabetes, this dual incretin co-agonist more effectively lowered body fat and corrected hyperglycemia than selective mono-agonists for the GLP-1 and GIP receptors. An enhanced insulinotropic effect translated from rodents to monkeys and humans, with substantially improved levels of glycosylated hemoglobin A_{1c} (HbA_{1c}) in humans with type 2 diabetes. The dual incretin was engineered with selective chemical modifications to enhance pharmacokinetics. This, in combination with its inherent mixed agonism, lowered the drug dose and ameliorated the dose-limiting nausea that has plagued selective GLP-1 therapies. These dual incretin co-agonists signify a new direction for unimolecular combination therapy and represent a new class of drug candidates for the treatment of metabolic diseases.

Science Translational Medicine (print ISSN 1946-6234; online ISSN 1946-6242) is published weekly, except the last week in December, by the American Association for the Advancement of Science, 1200 New York Avenue NW, Washington, DC 20005.

OBESITY

Unimolecular Dual Incretins Maximize Metabolic Benefits in Rodents, Monkeys, and Humans

Brian Finan,[1,2,3]* Tao Ma,[3,4]* Nickki Ottaway,[5] Timo D. Müller,[1,2] Kirk M. Habegger,[5] Kristy M. Heppner,[5] Henriette Kirchner,[6] Jenna Holland,[5] Jazzminn Hembree,[5] Christine Raver,[5] Sarah H. Lockie,[7] David L. Smiley,[3] Vasily Gelfanov,[3] Bin Yang,[3,8] Susanna Hofmann,[2] Dennis Bruemmer,[9] Daniel J. Drucker,[10] Paul T. Pfluger,[1,2,5] Diego Perez-Tilve,[5] Jaswant Gidda,[8] Louis Vignati,[8] Lianshan Zhang,[8] Jonathan B. Hauptman,[11] Michele Lau,[11] Mathieu Brecheisen,[11] Sabine Uhles,[11] William Riboulet,[11] Emmanuelle Hainaut,[11] Elena Sebokova,[11] Karin Conde-Knape,[11] Anish Konkar,[11] Richard D. DiMarchi,[3†] Matthias H. Tschöp[1,2,5†]

We report the discovery and translational therapeutic efficacy of a peptide with potent, balanced co-agonism at both of the receptors for the incretin hormones glucagon-like peptide-1 (GLP-1) and glucose-dependent insulinotropic polypeptide (GIP). This unimolecular dual incretin is derived from an intermixed sequence of GLP-1 and GIP, and demonstrated enhanced antihyperglycemic and insulinotropic efficacy relative to selective GLP-1 agonists. Notably, this superior efficacy translated across rodent models of obesity and diabetes, including *db/db* mice and ZDF rats, to primates (cynomolgus monkeys and humans). Furthermore, this co-agonist exhibited synergism in reducing fat mass in obese rodents, whereas a selective GIP agonist demonstrated negligible weight-lowering efficacy. The unimolecular dual incretins corrected two causal mechanisms of diabesity, adiposity-induced insulin resistance and pancreatic insulin deficiency, more effectively than did selective mono-agonists. The duration of action of the unimolecular dual incretins was refined through site-specific lipidation or PEGylation to support less frequent administration. These peptides provide comparable pharmacology to the native peptides and enhanced efficacy relative to similarly modified selective GLP-1 agonists. The pharmacokinetic enhancement lessened peak drug exposure and, in combination with less dependence on GLP-1–mediated pharmacology, avoided the adverse gastrointestinal effects that typify selective GLP-1–based agonists. This discovery and validation of a balanced and high-potency dual incretin agonist enables a more physiological approach to management of diseases associated with impaired glucose tolerance.

INTRODUCTION

Obesity and its associated comorbidities, especially adult-onset diabetes, are rapidly approaching worldwide epidemic levels. Management of such diseases through changes in life-style typically fails for multiple reasons. Consequently, a reliable therapeutic intervention that is less invasive than bariatric surgery is urgently needed. Current pharmacological antiobesity treatments have often been plagued by low efficacy and unacceptable side effects. Incretin-based therapy offers the promise to address both of these limitations. By simultaneously targeting at least two causal mechanisms of obesity-linked diabetes, insulin resistance and insulin deficiency, this approach has superior potential for the treatment of diabetes and obesity. Furthermore, the absence of adverse cardiovascular side effects or neuropsychological complications favorably segregates incretin-based drugs from the more classical small molecule–based approaches.

Incretins are endogenous peptide hormones, with glucagon-like peptide-1 (GLP-1) and glucose-dependent insulinotropic polypeptide (GIP) being the most well studied. Both hormones are secreted from the intestine in response to ingested nutrients and lower postprandial glucose excursion through insulinotropic actions at pancreatic β cells. GLP-1 also suppresses appetite, resulting in reduced adiposity (*1*, *2*). Treatment with GLP-1 receptor (GLP-1R) agonists provides sizable glycemic benefits without hypoglycemic risk, as well as meaningful improvements in body weight (*3*). Although currently approved GLP-1R agonists (exenatide and liraglutide) can convey such metabolic improvements, long-term glucose control is still less than perfect and reductions in adiposity remain far below that desired by patients and physicians (*4*). Increasing the dose to gain greater efficacy is not a viable option for most patients because GLP-1R agonists are a source of significant gastrointestinal side effects, most notably nausea and vomiting. Therefore, combination therapy appears to be the preferred path to enhanced efficacy while maintaining an appropriate tolerability and safety profile.

GLP-1 is widely regarded as the incretin of therapeutic utility, whereas GIP has been discounted for multiple reasons. GIP receptor (GIPR) agonism is purported to have pro-obesity effects (*5*–*11*), and its antihyperglycemic pharmacology is sharply diminished in diabetic patients (*12*, *13*). Nonetheless, dipeptidylpeptidase IV (DPP-IV) inhibitors increase endogenous levels of both GLP-1 and GIP and serve to improve

[1]Institute for Diabetes and Obesity, Helmholtz Zentrum München, German Research Center for Environmental Health (GmbH), Neuherberg 85764, Germany. [2]Division of Metabolic Diseases, Department of Medicine, Technische Universität München, Munich 80333, Germany. [3]Department of Chemistry, Indiana University, Bloomington, IN 47405, USA. [4]Research Center, Beijing Hanmi Pharmaceutical, Beijing 10131, China. [5]Metabolic Diseases Institute, Division of Endocrinology, Department of Internal Medicine, University of Cincinnati College of Medicine, Cincinnati, OH 45237, USA. [6]Department of Molecular Medicine and Surgery, Karolinska Institute, Stockholm 17177, Sweden. [7]Department of Physiology, Monash University, Melbourne, Victoria 3800, Australia. [8]Marcadia Biotech, Carmel, IN 46032, USA. [9]Saha Cardiovascular Research Center, University of Kentucky College of Medicine, Lexington, KY 40536, USA. [10]Department of Medicine, Samuel Lunenfeld Research Institute, Mt. Sinai Hospital, University of Toronto, Toronto, Ontario M5G 1X5, Canada. [11]F. Hoffmann–La Roche Ltd., Basel 4070, Switzerland.
*These authors contributed equally to this work.
†Corresponding author. E-mail: rdimarch@indiana.edu (R.D.D.); tschoep@helmholtz-muenchen.de (M.H.T.)

glucose control and insulin sensitivity without weight gain. More recent evidence shows that overexpression of GIP leads to improved body weight and glycemic control, contradicting the notion that GIP is obesogenic (*14*). Furthermore, genetic impairment of GIP signaling at pancreatic β cells in pigs demonstrated a pathobiology that replicates the development of adult-onset diabetes in humans, without any apparent change in body weight (*15*).

One strategy to enhance the efficacy of GLP-1 agonists includes its coadministration with other endogenous hormones (*16*–*18*). Acute co-infusion of GLP-1 and GIP in diabetic patients resulted in an enhanced first-phase insulin secretory response (*19*). Although coadministration provides maximal flexibility in a research setting, it is inherently more complex to develop as a medicine. A single molecule with balanced, mixed agonism is much simpler for the patient and the prescribing physician. However, the synthetic challenge in identifying single peptides of optimal balance and proving their unique pharmacology is often a big technical challenge. We have recently reported the development of single-molecule peptides that have balanced GLP-1R and glucagon receptor (GCGR) co-agonism (*20*). They potently and effectively reversed diet-induced obesity and insulin resistance in rodents, with the GLP-1 agonism eliminating the inherent diabetogenic liability of glucagon agonism. Glycemic improvements in this paradigm are associated with considerable weight loss. The rodent-to-human translation of these glucagon-based co-agonists remains to be fully characterized, but recent evidence suggests an appropriate acute tolerability (*21*). Here, our goal was to maximize glycemic outcomes through combination therapy, and we hypothesized that GIP could be recruited as a nonredundant partner with GLP-1 to generate unimolecular dual incretin agonists of superior efficacy. Ultimately, we envisioned that this incretin marriage would enhance the metabolic efficacy and therapeutic index of selective GLP-1 therapy.

We report herein the discovery of unimolecular, dual incretin co-agonists with balanced activity at each constitutive receptor and optimized pharmacokinetics. They potently reversed the metabolic syndrome through synergistic pharmacology, including an enhanced effect on adiposity, hyperglycemia, and dyslipidemia in rodent models of obesity, insulin resistance, and type 2 diabetes, compared to best-in-class selective GLP-1 agonists. We demonstrate that these GLP-1/GIP co-agonists improve glucose homeostasis through a potent effect on acute glucose-stimulated insulin release in rodents, and show that this insulinotropic effect translates to cynomolgus monkeys and humans, ultimately resulting in improved levels of glycosylated hemoglobin A_{1c} (HbA_{1c}) in type 2 diabetic patients. Unlike GLP-1R mono-agonist therapy, the co-agonists did not induce adverse gastrointestinal effects in humans. Collectively, the discovery and validation of these dual incretin peptides provides a fresh perspective on GIP pharmacology for treating metabolic diseases and offers a new direction for enhancing the efficacy of selective GLP-1R agonists to generate better drug candidates for the treatment of type 2 diabetes, obesity, and associated comorbidities.

RESULTS

GLP-1 and GIP analog coadministration enhances weight-lowering efficacy

To determine whether GLP-1 and GIP coadministration would result in additive effects on adiposity and glycemia, we compared their equimolar coadministration to individual administration of GLP-1 and GIP analogs in diet-induced obese (DIO) mice. We chose a dose at which, compared to vehicle, the GIP analog did not cause significant metabolic improvements. A comparable dose of a GLP-1 analog decreased body weight by 15.4% [61.4 ± 1.2 g to 51.9 ± 1.1 g ($P < 0.001$, $n = 8$ mice per group)] (Fig. 1A), reduced food intake (Fig. 1B), and prevented fat mass accumulation (Fig. 1C). However, coadministration decreased body weight by 20.8% (62.3 ± 1.4 g to 49.4 ± 1.2 g, $P < 0.001$) (Fig. 1A), reduced food intake ($P < 0.001$) (Fig. 1B), and decreased fat mass ($P < 0.001$) (Fig. 1C) to a greater extent than either mono-agonist alone. Coadministration did not, however, potentiate the glucose-lowering effect of either mono-agonist in ad libitum–fed mice (Fig. 1D), demonstrating that maximal glycemic benefits in these insulin-resistant, nondiabetic mice could be achieved by mono-agonism, at least at the doses tested here. Collectively, these results demonstrated that the combination of GIP and GLP-1 pharmacology potentiated the benefits of GLP-1 on adiposity despite GIP alone having negligible effects, and served as the rationale to pursue single-molecule co-agonists of GLP-1 and GIP.

Generating a highly potent peptide with balanced agonism at both the GLP-1R and GIPR

On the basis of the enhanced efficacy of GLP-1 and GIP coadministration, we investigated the potential of engineering a single-molecule GLP-1/GIP co-agonist. The structural similarities between GLP-1 and GIP, coupled with previous structure-activity insights, guided the rational design of sequence intermixed peptides of potent and balanced co-agonism. Intermediary candidates were built from a glucagon-based core sequence with residues incorporated from GLP-1 that were previously shown to impart balanced and potent co-agonism at GCGR and GLP-1R (Table 1, compound 10) (*20*). Our present objective was to provide balanced activity at the GLP-1R and GIPR while minimizing activity at the GCGR. Here, a series of peptide analogs was progressed in a stepwise manner starting with the previously validated GLP-1/glucagon co-agonist (*20*). Each peptide was subsequently tested for its ability to activate human GLP-1R, GIPR, and GCGR in a cell-based reporter gene assay for cyclic adenosine monophosphate (cAMP) induction. The full sequences for each peptide in Table 1 can be found in fig. S1.

Selectivity for the respective incretin receptors was hypothesized to arise from sequence differences in the middle and C-terminal regions; thus, GIP-specific residues were introduced to the region between the lactam bridge at residues 16 and 20 (Table 1, compound 10) (*20*). However, substitution of GIP-specific residues Ile^{17}, His^{18}, and Gln^{19} failed to enhance GIP activity (Table 1, compound 11). We next made selective modifications to the C-terminal portion of peptide 10. Because exclusion of the C-terminal portion of native GIP does not influence activity at the human GIPR, we added the C-terminally extended (Cex) residues from exendin-4 in an attempt to gain dual incretin activity. This addition further exacerbated GIP activity (Table 1, compound 12), but this reduction in GIP activity was prevented by substitution with GIP-specific Tyr^1 (Table 1, compound 13). Further modification to the C terminus by substitution with Val^{23}, Asn^{24}, Leu^{27}, and Ala^{28} substantially increased GIP activity, with only modest changes in glucagon or GLP-1 activity (Table 1, compound 14). Substitution with GIP-derived Ile^{12}, along with aminoisobutyric acid (Aib) at position 2, provided an analog with enhanced incretin activity at the expense of glucagon activity (Table 1, compound 15). In addition to blunting glucagon activity, Aib at position 2 prevented physiological degradation and inactivation by DPP-IV. However, peptide 15 was unbalanced at the incretin receptors and retained significant residual glucagon activity. Glucagon activity

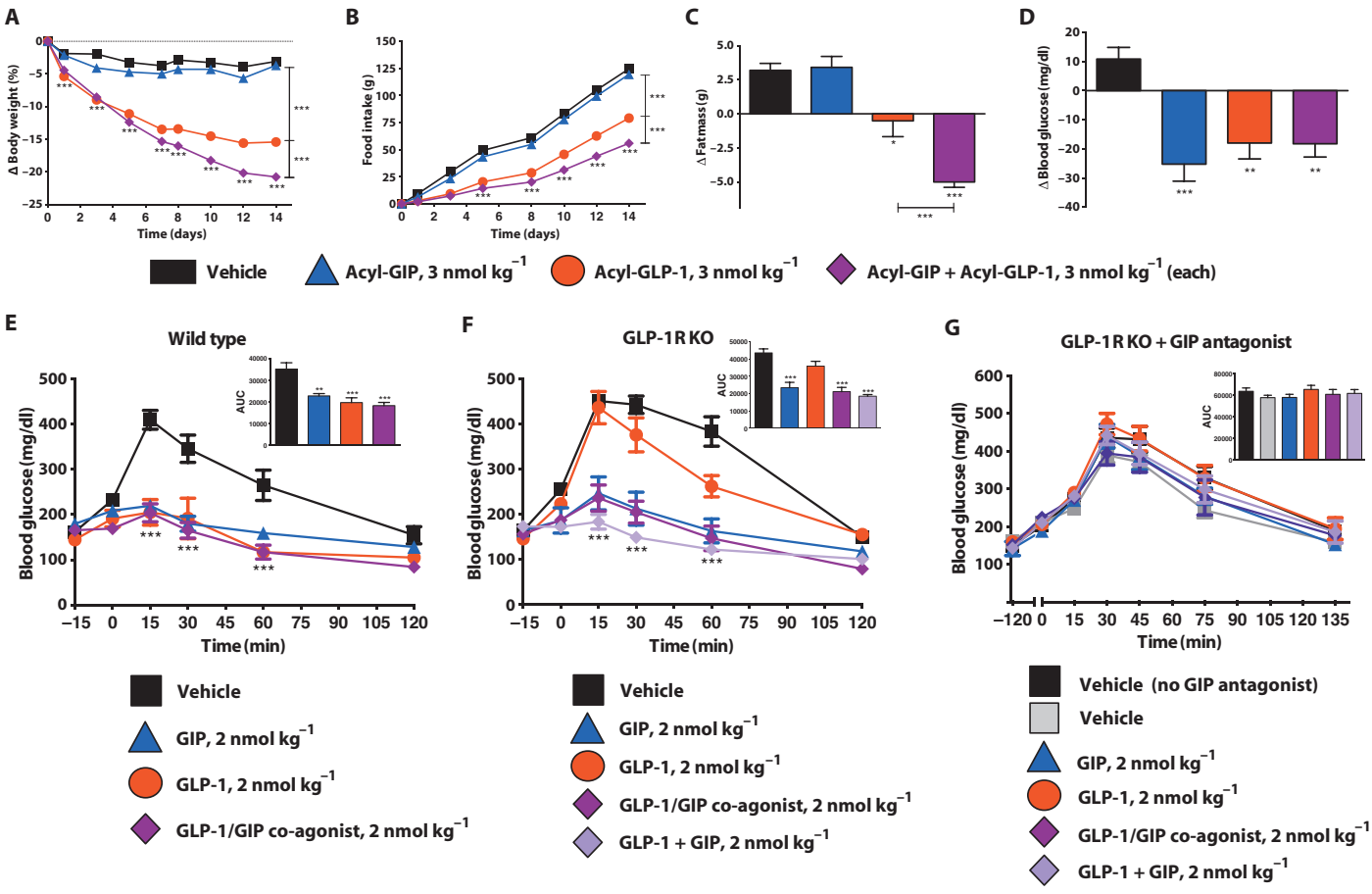

Fig. 1. Incretin coadministration enhances metabolic outcomes and demonstration of in vivo co-agonism. (**A** to **D**) Two-week treatment of DIO male mice with incretin mono-agonists. Effects on (A) body weight, (B) cumulative food intake, (C) fat mass, and (D) ad libitum–fed blood glucose (n = 8) after daily subcutaneous injections of saline (black), a GIP agonist (Table 1, compound 6, blue), a GLP-1 agonist (Table 1, compound 3, red), and the coadministration of the GIP and GLP-1 mono-agonists (purple) at a dose of 3 nmol/kg for each. (**E** to **G**) Acute treatment of DIO male mice with incretin mono- and co-agonists. Effects on intraperitoneal glucose tolerance after a single intraperitoneal injection 15 min before glucose challenge (n = 8) of saline (black), a GIP mono-agonist (Table 1, compound 6, blue), a GLP-1 mono-agonist (Table 1, compound 3, red), the coadministration of the GIP and GLP-1 mono-agonists (light purple/violet), and an engineered GLP-1/GIP co-agonist (Table 1, compound 18, dark purple/plum) at a dose of 2 nmol/kg. Glucose tolerance in (E) wild-type DIO mice, (F) GLP-1R$^{-/-}$ DIO mice, and (G) GLP-1R$^{-/-}$ DIO mice pretreated with a GIPR antagonist 2 hours before glucose challenge at a dose of 2.25 μmol/kg. Data in (A) to (G) represent means ± SEM. *P < 0.05, **P < 0.01, ***P < 0.001, determined by analysis of variance (ANOVA) comparing vehicle to compound injections unless otherwise noted. AUC, area under the curve.

is dependent on lactam-induced helix stabilization in the middle region of the GLP-1/glucagon co-agonist (*20*). We therefore removed the lactam bridge and introduced Aib at position 20. These simultaneous changes induced stabilization of the helix to a lesser degree than the lactam bond. Additionally, a C-terminal residue (Cys^{40}) was added to serve as an anchor for subsequent modification with polyethylene glycol (PEG) or fatty acids, as necessary. The resulting analog (Table 1, compound 16) had balanced and potent activities at the two incretin receptors and a glucagon activity that was 1% that of native glucagon. Substitution with GIP-derived residues Glu^{3} and Lys^{16} resulted in an analog with appropriately balanced and potent activity at both GLP-1R and GIPR, with almost no in vitro glucagon activity (Table 1, compound 17).

This resulting peptide sequence served as the backbone for engineering the balanced and potent dual incretin co-agonists with optimized pharmacokinetics. The C-terminal anchor had little effect on receptor activity and could be substituted with Lys^{40} to facilitate amide linkage of a fatty acid (Table 1, compound 18). This peptide served as the unimolecular dual incretin subsequently studied in vivo and compared to exendin-4. Direct lipidation with a 16-carbon acyl chain (16:0) through Lys^{40} resulted in a uniform increase in activity at all three receptors. This analog has superior potency (>500%) at both incretin receptors, and 2% of the activity of native glucagon (Table 1, compound 19). It served as the acylated unimolecular dual incretin in subsequent in vivo studies and compared to liraglutide. Previously, position 24 was identified as a site that can facilitate site-specific PEG addition (PEGylation) (*20*). Here, Cys^{24} substitution was confirmed to have a negligible effect on the constitutive receptor activity profile (Table 1, compound 20). Site-specific 40-kD PEGylation at Cys^{24} reduced receptor activity at all three receptors, but activity at both incretin receptors remained balanced with subnanomolar potency. This analog also had an activity at GCGR that was less than 0.02% of native glucagon (Table 1, compound 21). This

Table 1. In vitro GLP-1R, GIPR, and GCGR activity of peptide analogs. EC_{50} values represent the effective peptide concentrations (nM) that stimulate half-maximum activation at the GLP-1R, GIPR, and GCGR. A minimum of three separate experiments was conducted for each analog at each respective receptor. Relative % activity at each receptor = (native ligand EC_{50}/analog EC_{50}) × 100. Underlined residues in peptide 10 represent residues featuring a side-chain lactam bridge. Peptides 11 to 21 feature the same sequence as the proceeding analog with the subsequent modification depicted in parentheses, with the exception of peptide 20, which was designed from parent peptide 18. All sequences are found in fig. S1.

No.	Analog	GLP-1R			GIPR			GCGR		
		EC_{50} (nM)	SD	Relative GLP-1 %	EC_{50} (nM)	SD	Relative GIP %	EC_{50} (nM)	SD	Relative glucagon %
1	GLP-1	0.028	0.002	100	1513.825	78.950	0	2449.288	106.460	0
2	Exendin-4	0.004	0.001	621	2.952	0.841	1	186.147	16.677	0
3	GLP-1 (Aib^2 E^{16} Cex K^{40})	0.017	0.003	158	1200.336	100.003	0	2000.659	500.000	0
4	Liraglutide	0.011	0.003	249	78.657	7.620	0	172.929	22.561	0
5	GIP	1567.012	65.780	0	0.020	0.004	100	417.480	10.370	0
6	GIP (Aib^2)	3527.099	310.810	0	0.016	0.001	126	1459.502	123.800	0
7	GIP (Aib^2 Cex K^{40}-C_{16} acyl)	6.330	2.690	0	0.012	0.001	168	2.920	0.840	1
8	Glucagon	3.100	0.494	1	1538.109	329.020	0	0.032	0.006	100
9	Glucagon (Aib^2 K^{10}-γEγE-C_{16} acyl Aib^{20})	0.479	0.068	6	22.650	6.100	0	0.005	0.001	616
10	Glucagon ($\underline{E}^{16}$ Q^{17} A^{18} $\underline{K}^{20}$ E^{21} I^{23} A^{24})-NH_2	0.022	0.002	126	6.258	1.278	0	0.030	0.009	104
11	Peptide 10 (I^{17} H^{18} Q^{19})-NH_2	0.140	0.019	20	5.530	1.099	0	0.150	0.022	21
12	Peptide 11 (Q^{17} A^{18} A^{19} Cex)-NH_2	0.020	0.002	138	14.557	2.241	0	0.060	0.003	53
13	Peptide 12 (Y^1)-NH_2	0.120	0.008	23	3.054	0.663	1	0.060	0.003	53
14	Peptide 13 (V^{23} N^{24} L^{27} A^{28})-NH_2	0.040	0.001	69	0.557	0.069	4	0.040	0.002	79
15	Peptide 14 (Aib^2 I^{12})-NH_2	0.010	0.001	276	0.176	0.019	11	0.190	0.039	17
16	Peptide 15 (Aib^{20} (–)lactam C^{40})-NH_2	0.024	0.009	115	0.040	0.007	50	3.457	0.699	1
17	Peptide 16 (E^3 K^{16})-NH_2	0.012	0.002	230	0.003	0.001	673	58.947	8.284	0
18	Peptide 17 (K^{40})-NH_2	0.016	0.002	177	0.010	0.002	202	6.908	1.586	0
19	Peptide 18 (K^{40}-C_{16} acyl)-NH_2	0.005	0.001	509	0.003	0.001	691	1.286	0.103	2
20	Peptide 18 (C^{24})-NH_2	0.024	0.004	117	0.006	0.001	337	12.192	1.433	0
21	Peptide 20 (C^{24}-40 kD PEG)-NH_2	0.323	0.028	9	0.194	0.043	10	358.500	44.770	0

analog served as the PEGylated unimolecular dual incretin used in subsequent in vivo studies.

A unimolecular dual incretin improves glucose tolerance through GLP-1R– and GIPR-dependent mechanisms

We confirmed that the balanced in vitro potency of the co-agonist translated to in vivo activity by comparing the acute effects on glucose tolerance in wild-type DIO mice versus mice with genetically silenced GLP-1R signaling, pharmacologically silenced GIPR signaling, or the combination thereof. In wild-type DIO mice, both GLP-1 and GIP mono-agonists and the co-agonist improved glucose tolerance to a similar extent (Fig. 1E). In GLP-1R knockout (GLP-1RKO) mice, the GLP-1 analog failed to recapitulate the improvements in glucose tolerance observed in the wild-type mice, whereas the GIP analog, the co-agonist peptide, and the coadministration of both mono-agonists all similarly improved glucose tolerance (Fig. 1F). This demonstrates that the co-agonist peptide had in vivo GIP activity, which had a potent effect on improving glycemic control.

To establish that GLP-1 activity is also present in the co-agonist peptide, we pretreated the GLP-1RKO mice with a GIPR antagonist to generate a GLP-1R and GIPR loss-of-function model, essentially mimicking dual incretin receptor knockout (DIRKO) mice (*22*). In this setting, both of the mono-agonists, individually or in combination, as well as the co-agonist peptide failed to improve glucose tolerance (Fig. 1G). The results of this reductionist approach demonstrated that our co-agonist peptide had sufficient and comparable in vivo activity at both receptors, in the context of acute glycemic control, and validated it as a GLP-1/GIP co-agonist. Furthermore, the results demonstrated that the co-agonist did not have additional off-target pharmacology that might contribute to its glucoregulatory efficacy.

A unimolecular dual incretin is more effective at improving systemic metabolism than exendin-4

To determine whether enhanced metabolic improvements can be gained by chronic treatment with the GLP-1/GIP co-agonist compared to a GLP-1R mono-agonist alone, we compared escalating doses of the unacylated/free peptide co-agonist (Table 1, compound 18) to equimolar doses of exendin-4 in DIO mice. The co-agonist stimulated a dose-dependent decrease in body weight (Fig. 2A), food intake (Fig. 2B), fat mass (Fig. 2C), and ad libitum–fed blood glucose (Fig. 2D). The metabolic efficacy of the co-agonist was significantly greater than that of exendin-4, which had negligible or minimal effects on these metabolic parameters at the same dose. At the highest dose studied (30 nmol/kg), the co-agonist decreased body weight by 14.0% [57.6 ± 0.8 g to 49.5 ± 0.9 g ($P < 0.001$, $n = 8$ per group)], whereas exendin-4 decreased body weight by only 3.5% (57.8 ± 1.4 g to 55.8 ± 1.4 g, $P < 0.001$) (Fig. 1A). Additionally, mice treated with this dose of the co-agonist displayed reduced food intake, fat mass, and ad libitum–fed blood glucose compared to exendin-4–treated mice (Fig. 2, B to D). Notably, only 10% of the dose of the co-agonist was required to achieve modest weight loss comparable to that induced by exendin-4 alone. Collectively, these results demonstrate that greater metabolic efficacy can be gained by treatment with a dual incretin agonist compared to a best-in-class GLP-1 mono-agonist, and that chronic GIP agonism does not aggravate adiposity when supplemented with GLP-1 agonism.

An acylated unimolecular dual incretin is more effective at improving systemic metabolism than liraglutide

To achieve a GLP-1/GIP co-agonist with a more favorable pharmacokinetic profile that allows for less frequent dosing, we acylated the co-agonist peptide with palmitic acid (C16:0). We directly acylated the peptide at a C-terminal lysine residue, which was confirmed to not have any appreciable influence on the inherent in vitro potency, co-agonism balance, or selectivity at the GLP-1R, GIPR, or GCGR [$EC_{50\ GLP\text{-}1R}$ = 0.005 ± 0.001 nM, $EC_{50\ GIPR}$ = 0.003 ± 0.001 nM, $EC_{50\ GCGR}$ = 1.286 ± 0.103 nM (Table 1, compound 19)].

To determine whether similarly enhanced metabolic improvements were gained with an acylated GLP-1/GIP co-agonist, we compared escalating doses of the acylated dual incretin (Table 1, compound 19) to

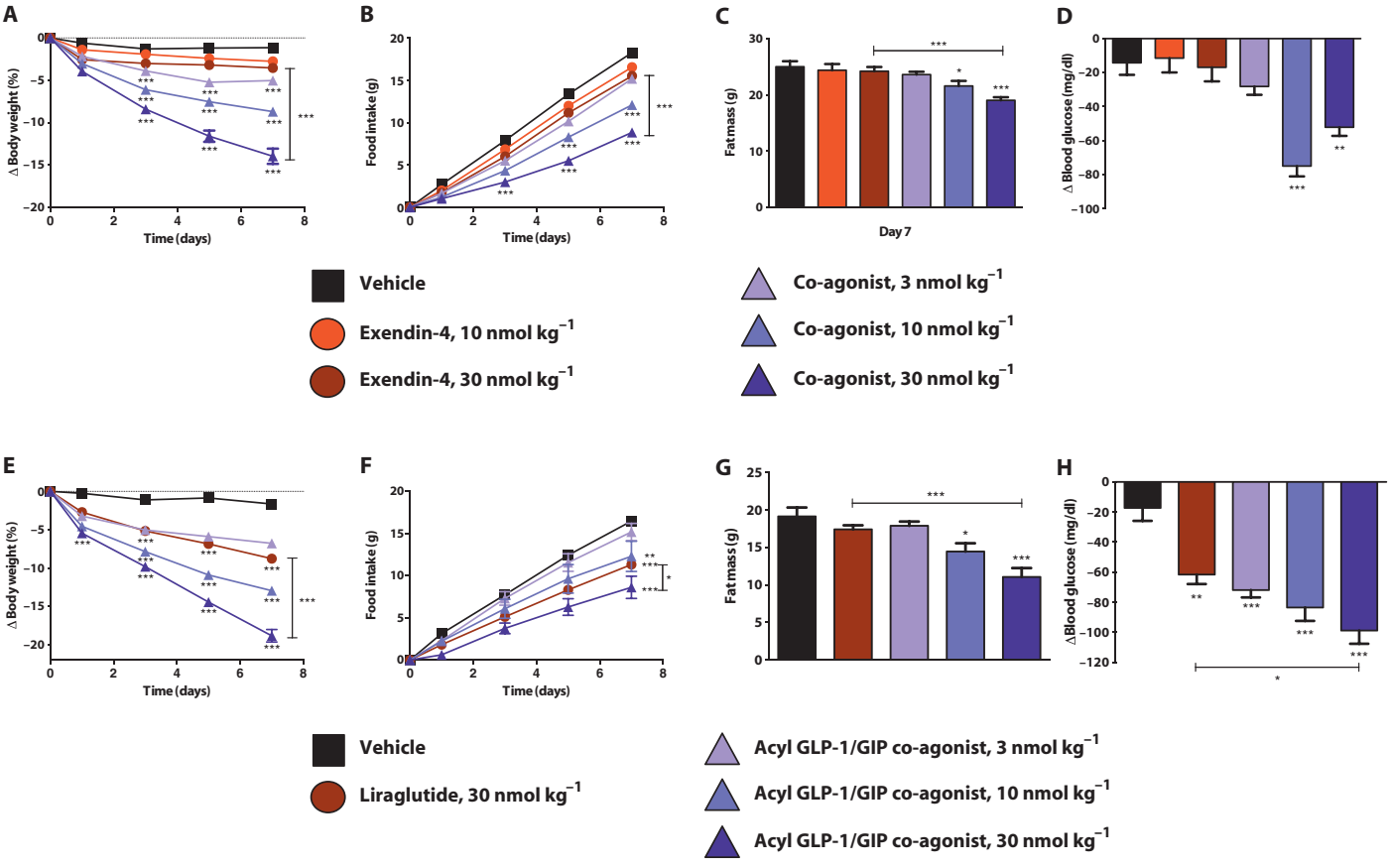

Fig. 2. Unimolecular dual incretins enhance metabolic outcomes compared to GLP-1R agonists. (**A** to **D**) One-week treatment of DIO male mice with free peptide versions of a GLP-1 mono-agonist and GLP-1/GIP co-agonist. Effects on (A) body weight, (B) cumulative food intake, (C) fat mass, and (D) ad libitum–fed blood glucose ($n = 8$) after daily subcutaneous injections of saline (black), exendin-4 (red), and a GLP-1/GIP co-agonist (Table 1, compound 18, purple) at two different doses: 10 nmol/kg (lighter shade) and 30 nmol/kg (darker shade). (**E** to **H**) One-week treatment of DIO male mice with acylated versions of a GLP-1 mono-agonist and GLP-1/GIP co-agonist. Effects on (E) body weight, (F) cumulative food intake, (G) fat mass, and (H) ad libitum–fed blood glucose ($n = 8$) after daily subcutaneous injections of saline (black), liraglutide (red) at a single dose of 30 nmol/kg, and an acylated GLP-1/GIP co-agonist (Table 1, compound 19, purple) at three different doses: 3, 10, and 30 nmol/kg (lighter to darker shade). Data in (A) to (H) represent means ± SEM. *$P < 0.05$, **$P < 0.01$, ***$P < 0.001$, determined by ANOVA comparing vehicle to compound injections unless otherwise noted.

an acylated GLP-1 analog (liraglutide) in DIO mice. Comparable to the free peptide co-agonist, the acylated co-agonist decreased body weight (Fig. 2E), food intake (Fig. 2F), fat mass (Fig. 2G), and ad libitum–fed blood glucose (Fig. 2H) in a dose-dependent manner. The metabolic improvements evinced by the acylated co-agonist were enhanced compared to an equimolar dose of liraglutide. At the maximum dose tested (30 nmol/kg), the acylated co-agonist reduced body weight by 18.8% [48.2 ± 1.5 g to 39.1 ± 1.5 g ($P < 0.001$, $n = 8$)], whereas liraglutide decreased body weight by only 8.8% [47.0 ± 1.2 g to 43.8 ± 0.8 g ($P < 0.001$, $n = 8$)] (Fig. 2E). Furthermore, the acylated co-agonist amplified the effect on food intake ($P < 0.05$) (Fig. 2F), fat mass ($P < 0.001$) (Fig. 2G), and blood glucose ($P < 0.05$) (Fig. 2H) compared to the equivalent dose of liraglutide. Much like the unacylated co-agonist, similar metabolic improvements can be achieved with the acylated co-agonist at 10% of the dose of liraglutide. At 3 nmol/kg, the acylated co-agonist decreased body weight by 6.8% (48.8 ± 1.1 g to 45.5 ± 1.2 g, $P < 0.001$) (Fig. 2E) and blood glucose by 71.9 mg/dl ($P < 0.001$) (Fig. 2H), which are changes comparable to the improvements induced by the 10-fold higher dose of liraglutide. This suggested that the difference was inherent to the peptide and not a function of pharmacokinetics.

To determine whether the potentiated efficacy of the co-agonist could be sustained with less-frequent chronic dosing, we administered the same acylated co-agonist or liraglutide as biweekly injections to DIO mice for 4 weeks. Much like daily dosing, biweekly administration of the acylated co-agonist resulted in a dose-dependent reduction in body weight (Fig. 3A), food intake (Fig. 3B), and fat mass (Fig. 3C). Furthermore, the biweekly administration of the acylated co-agonist improved glucose tolerance (Fig. 3, D and E) and lowered plasma insulin (Fig. 3F) and cholesterol levels (Fig. 3G). Likewise, this biweekly dosing regimen of the acylated co-agonist resulted in greater and sustained metabolic improvements compared to a similar dosing pattern of liraglutide. At the higher dose (20 nmol/kg), the acylated co-agonist decreased body weight by 21.5% [62.3 ± 0.8 g to 48.9 ± 1.3 g ($P < 0.001$, $n = 8$ each group)] (Fig. 3A), whereas liraglutide failed to induce any weight loss compared to vehicle controls. Furthermore, this dose of the acylated co-agonist significantly decreased cumulative food intake (Fig. 3B; $P < 0.001$) and fat mass (Fig. 3C; $P < 0.001$), improved glucose tolerance (Fig. 3, D and E; $P < 0.001$), and decreased circulating cholesterol levels (Fig. 3G; $P < 0.01$) compared to liraglutide, which failed to induce any improvements in these metabolic parameters.

Given that the co-agonist reduced food intake, anorectic or satiation mechanisms appeared to contribute to the negative energy balance, leading to the robust weight loss. However, the co-agonist did not demonstrate any significant effect on energy expenditure, respiratory quotient, or locomotor activity (fig. S2, A to C). To assess whether the control of food intake is the sole factor driving the body weight changes, we compared the acylated co-agonist to pair-fed control mice. At the higher dose (30 nmol/kg), the acylated co-agonist decreased body weight by 24.7% [51.6 ± 1.7 g to 38.9 ± 1.5 g ($P < 0.001$ to vehicle, $n = 8$)], whereas pair-feeding to this dose decreased body weight by only 18.6% (51.5 ± 1.5 g to 41.9 ± 1.4 g, $P < 0.001$) (fig. S3, A to C). These pair-feeding results demonstrated that the acylated GLP-1/GIP co-agonist targets additional mechanisms that contribute to the benefits in body weight management that cannot solely be explained by decreased energy intake alone, which suggests improved feeding efficiency, increased thermogenesis, or malabsorption. However, extensive genetic profiling of adipose, liver, and muscle tissue

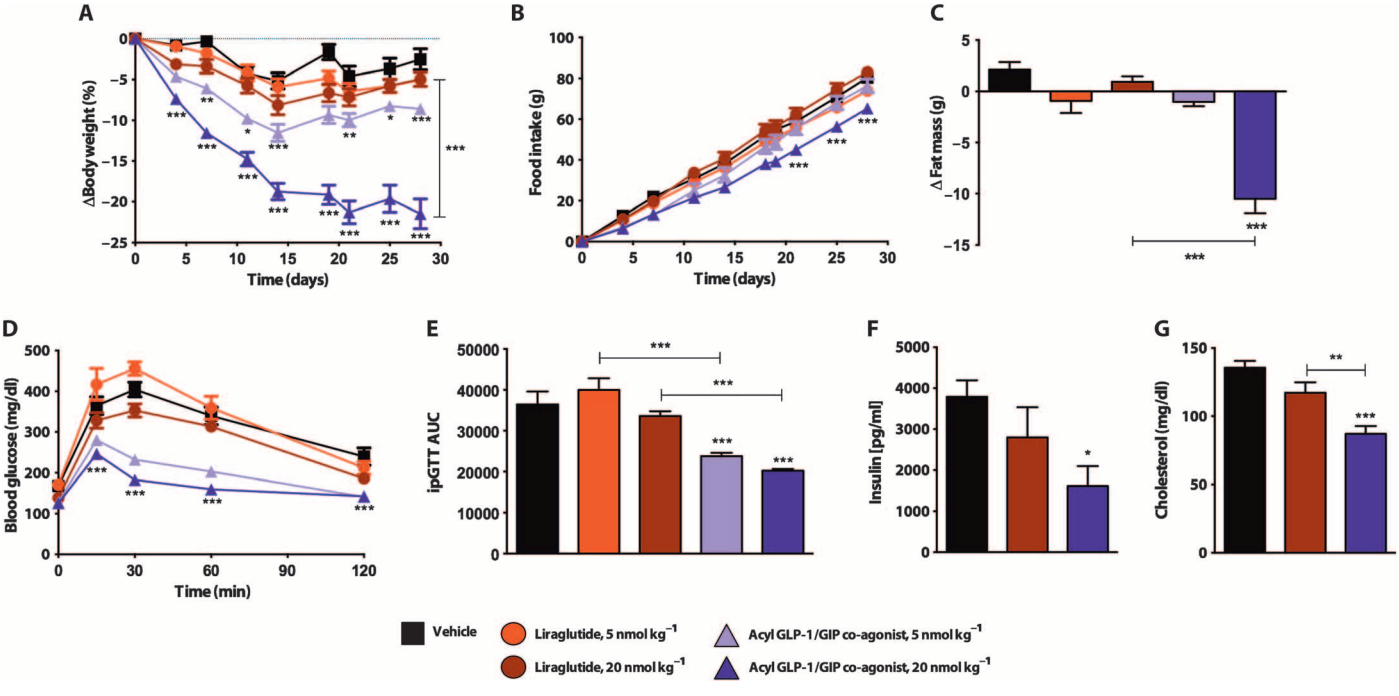

Fig. 3. Less frequent administration of a unimolecular dual incretin amplifies metabolic outcomes. (**A** to **G**) Four-week treatment of DIO male mice with biweekly doses of acylated versions of a GLP-1 mono-agonist and a GLP-1/GIP co-agonist. Effects on (A) body weight, (B) cumulative food intake, (C) fat mass, (D and E) intraperitoneal glucose tolerance (ipGTT), and plasma levels of (F) insulin and (G) total cholesterol ($n = 8$) after biweekly subcutaneous injections of saline (black), liraglutide (red), and an acylated GLP-1/GIP co-agonist (Table 1, compound 19, purple) at two different doses: 5 nmol/kg (lighter shade) and 20 nmol/kg (darker shade). Data in (A) to (G) represent means ± SEM. *$P < 0.05$, **$P < 0.01$, ***$P < 0.001$, determined by ANOVA comparing vehicle to compound injections unless otherwise noted.

did not reveal any changes in gene programs conferring altered inflammation, fatty acid use, lipid handling, or other metabolically relevant pathways (fig. S4, A to C). However, histological analysis of the epididymal white adipose tissue revealed that chronic treatment with the dual incretin co-agonist reduced the size of individual adipocytes compared to vehicle and liraglutide treatment (fig. S2D; $P < 0.001$).

To determine whether the acylated co-agonist has any additional off-target pharmacology, particularly residual glucagon activity, that could be a driving force behind the metabolic efficacy, we measured plasma markers indicative of chronic glucagon agonism. It is reasonable to suspect that if the co-agonist had alternative pharmacology contributing to its efficacy, glucagon would be a logical option because the co-agonist is a glucagon-based peptide despite negligible in vitro activity. The same acylated co-agonist did not increase plasma levels of fibroblast growth factor 21 (FGF21) (*23*) (fig. S2E) or plasma ketone levels in chronically treated DIO mice (fig. S2F). Additionally, we compared this acylated co-agonist to an acylated glucagon analog of comparable in vitro potency in global GLP-1RKO mice. In these mice, the acylated co-agonist demonstrated a blunted weight-lowering efficacy compared to the effect seen in wild-type mice. The acylated co-agonist lowered body weight only by 4.0% [54.0 ± 2.2 g to 51.9 ± 2.6 g ($P < 0.01$, n = 8 mice per group)] (fig. S5A), whereas the acylated glucagon agonist decreased body weight by 18.4% [53.9 ± 1.4 g to 44.0 ± 1.5 g ($P < 0.001$)] (fig. S5A). This difference in the weight-lowering efficacy argues against glucagon pharmacology as the basis for the metabolic benefits of the unimolecular dual incretin. In contrast to the weight-lowering effect, the glycemic efficacy was still evident with the co-agonist, but not with the glucagon analog. The acylated co-agonist lowered fasted blood glucose levels and improved glucose tolerance (fig. S5, D to F) compared to the acylated glucagon, which failed to improve glycemic control despite the robust weight loss, which is a function of its inherent hyperglycemic effect. Collectively, these results demonstrate that glucagon pharmacology is not driving the metabolic efficacy of the GLP-1/GIP co-agonist, and that the pharmacology of unimolecular dual incretins functions to improve glycemic control beyond the metabolic benefits indirectly derived from body weight loss.

Less frequent dosing of a PEGylated version of the co-agonist similarly improves systemic metabolism

To support less frequent dosing, another unimolecular dual incretin with more pronounced pharmacokinetic enhancement than conferred by acylation was achieved by attachment of a 40-kD PEG polymer to the co-agonist. To introduce a site for PEGylation, we introduced a cysteine residue at the 24th residue because this position was identified to have little influence on activity (Table 1, compound 21). The site-specific PEGylation via a maleimide linkage did not appreciably change the in vitro activity ratio at the three receptors compared to the free and acylated co-agonists despite a uniform reduction in potency ($EC_{50\ GLP\text{-}1R}$ = 0.323 ± 0.028 nM, $EC_{50\ GIPR}$ = 0.194 ± 0.043 nM, $EC_{50\ GCGR}$ = 358.5 ± 44.77 nM).

To determine whether less frequent dosing of the PEGylated co-agonist can match the robust efficacy observed in DIO mice with the acylated co-agonist, we compared equivalent weekly dosing of the acylated co-agonist (Table 1, compound 19) given daily to the PEGylated co-agonist (Table 1, compound 21) given weekly. Both the acylated and PEGylated co-agonists exceeded the weight-lowering effect of liraglutide (Fig. 4A), whereas all three compounds improved food intake, hyperglycemia, and dyslipidemia to comparable levels (Fig. 4, B to I). The acylated co-agonist lowered body weight by 31.4% [49.2 ± 1.0 g to 33.7 ± 0.6 g ($P < 0.001$, n = 8)] and the PEGylated co-agonist lowered body weight by 26.9% (47.5 ± 1.1 g to 34.7 ± 0.8 g, $P < 0.001$), whereas liraglutide only lowered body weight by 15.6% (47.5 ± 1.0 g to 40.1 ± 1.0 g, $P < 0.001$) (Fig. 4A). Both co-agonists also performed equally to reduce food intake (Fig. 4B), attenuate glucose intolerance (Fig. 4C), lower fasted blood glucose and plasma leptin (Fig. 4, D and E), and reduce plasma triglycerides (Fig. 4G). Unlike liraglutide, neither of the unimolecular dual incretins influenced plasma free fatty acid levels (Fig. 4H), suggesting that GIP counteracts the pharmacology of GLP-1 to increase circulating free fatty acids. All three compounds also improved liver function by reversing hepatic steatosis without hepatocellular toxicity, as reflected by the trend to lower serum alanine aminotransferase (ALT) and aspartate aminotransferase (AST) levels (fig. S6, A to C). Collectively, these results demonstrate that both of the pharmacokinetically optimized, unimolecular dual incretins improve systemic metabolism, including adiposity, hyperglycemia, and dyslipidemia, in DIO mice. The weight-lowering effects of these co-agonists are amplified compared to GLP-1 mono-agonist treatment, whereas blood glucose and lipid profiles were similarly improved in these nondiabetic mice. Because both of the co-agonists demonstrate similar pharmacology in DIO mice, they were each explored further in translational studies that included diabetic models.

Unimolecular dual incretins enhance insulinotropic effects compared to GLP-1 mono-agonism

To explore the prospect of enhanced insulinotropic efficacy of unimolecular dual incretins, we administered escalating doses of the PEGylated co-agonist to lean rats to assess the insulin response during a glucose challenge. Lean rats were used in this acute test to lessen the complications that might arise from prevailing islet failure or peripheral insulin resistance. Twenty-four hours after administration, the highest dose (20 nmol/kg) of the PEGylated co-agonist caused a significant reduction in the blood glucose profile compared to vehicle-treated controls (Fig. 5, A and B). The PEGylated co-agonist caused a dose-dependent increase in first-phase insulin secretion. At the highest dose, the PEGylated co-agonist significantly increased plasma insulin levels 10 min after the glucose challenge [6863 ± 727 pg/ml (n = 7, $P < 0.001$)] (Fig. 5C), which was also reflected in an increased plasma C-peptide level (Fig. 5D).

To determine whether the co-agonist provides an enhanced insulinotropic effect compared to GLP-1 mono-agonism, we made a similar comparison using an equimolar dose of the PEGylated co-agonist and an in vitro–matched PEGylated GLP-1 agonist. At a dose of 10 nmol/kg, the PEGylated versions of the co-agonist and GLP-1 agonist similarly improved glucose tolerance compared to vehicle (Fig. 5, E and F) in these euglycemic lean rats. However, the co-agonist increased acute plasma insulin [7194 ± 931 pg/ml (n = 8, $P < 0.05$)] (Fig. 5G) and the level of C-peptide (Fig. 5H) 10 min after glucose challenge, whereas the selective GLP-1 agonist did not change the insulin secretory response at this time point. Collectively, these results demonstrate that this co-agonist has a sustained insulinotropic activity after acute administration, and this activity is enhanced relative to a GLP-1 mono-agonist.

Unimolecular dual incretins enhance antihyperglycemic efficacy in diabetic rodent models compared to GLP-1 mono-agonism

Although DIO mice are a model for insulin resistance and glucose intolerance, they are not overtly hyperglycemic or diabetic. Therefore, we compared the antihyperglycemic efficacy of both the acylated and PEGylated co-agonists in *db/db* mice. We first tested the acute and

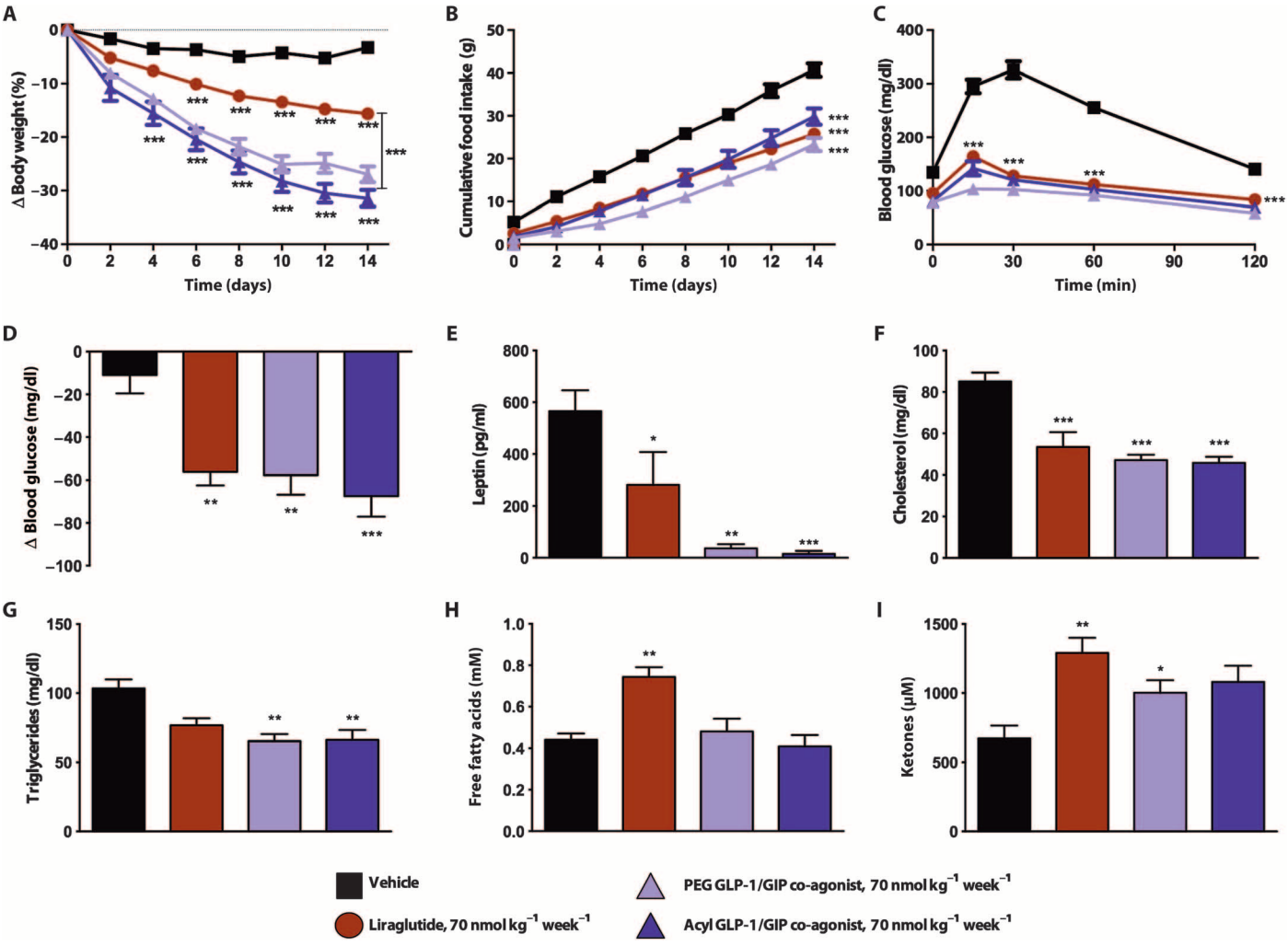

Fig. 4. Acylated and PEGylated versions of the co-agonist both amplify metabolic outcomes. (**A** to **I**) Two-week treatment of DIO male mice with acylated and PEGylated versions of GLP-1/GIP co-agonists. Effects on (A) body weight, (B) cumulative food intake, (C) intraperitoneal glucose tolerance, (D) fasting blood glucose, and plasma levels of (E) leptin, (F) total cholesterol, (G) triglycerides, (H) free fatty acids, and (I) ketones (n = 8) after daily subcutaneous injections of saline (black), liraglutide (red), and an acylated GLP-1/GIP co-agonist (Table 1, compound 19, dark purple) and weekly subcutaneous injections of a PEGylated GLP-1/GIP co-agonist at an equimolar weekly dose of 70 nmol/kg (Table 1, compound 21, light purple/violet). Data in (A) to (I) represent means ± SEM. *P < 0.05, **P < 0.01, ***P < 0.001, determined by ANOVA comparing vehicle to compound injections unless otherwise noted.

sustained ability of the dual incretins compared to liraglutide to improve glucose tolerance in *db/db* mice that received the compounds 24 hours before glucose challenge. Acutely, both of the co-agonists (Table 1, compounds 19 and 21) minimized the glucose excursion after a single injection, whereas an equimolar dose of liraglutide had no effect relative to vehicle (Fig. 6A). To test whether this potentiated effect on glycemic control is sustained after repeated administration, we gave liraglutide and both co-agonists (Table 1, compounds 19 and 21) to *db/db* mice at comparable doses to be consistent with experiments in DIO mice. At the administered doses, all three peptides prevented the excessive weight gain seen with control mice (Fig. 6B), similarly lowered fasted blood glucose levels (Fig. 6C), and similarly improved glycemic control (Fig. 6D), thus demonstrating a sufficient antihyperglycemic efficacy.

To assess the insulinotropic effect and subsequent effect on glycemic control, we compared both of the co-agonists to liraglutide in diabetic ZDF rats. At equivalent weekly doses, liraglutide and the co-agonists lowered fasted blood glucose levels with rapid onset and sustained efficacy (Fig. 6E), but only the co-agonists displayed a superior effect to lower HbA_{1c} and increased glycomark (a measure of 1,5-anhydroglucitol) compared to liraglutide (fig. S7, A and B). Furthermore, all three compounds were all capable of normalizing glucose tolerance (fig. S7C). However, treatment with both co-agonists required less insulin to normalize glucose tolerance when compared to liraglutide (fig. S7D). This decrease in insulin demand lessens the secretory burden of pancreatic β cells and suggests a parallel improvement in insulin sensitivity, as reflected by the improved HOMA-IR score (fig. S7E). Notably, the superior glycemic control induced by the co-agonists relative to liraglutide was independent of changes in body weight (fig. S7F), suggesting a direct effect on pancreatic islets. Histological analysis of the pancreas revealed that the co-agonists preserved proper islet cytoarchitecture (Fig. 6F), as reflected by a preservation of islet area (fig. S7G),

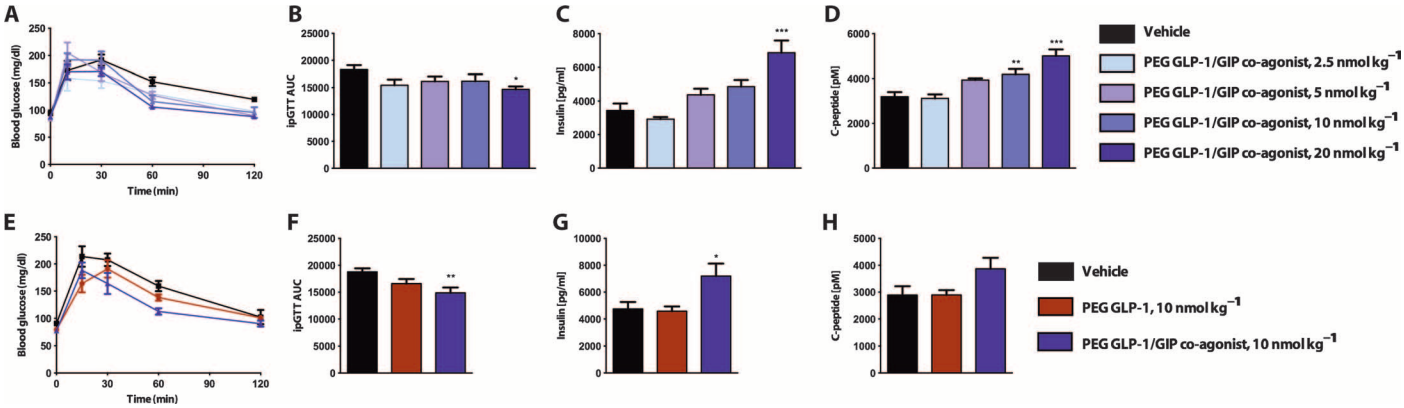

Fig. 5. Unimolecular dual incretins enhance insulinotropic response. (**A** to **D**) Acute treatment of lean male rats with a PEGylated GLP-1/GIP co-agonist. Effects on (A and B) intraperitoneal glucose tolerance and plasma levels of (C) insulin and (D) C-peptide 10 min after a glucose challenge (n = 8). Plasma analysis was performed 24 hours after the subcutaneous injection of saline (black) or a PEGylated GLP-1/GIP co-agonist (Table 1, compound 21, purple) at escalating doses of 2.5, 5, 10, and 20 nmol/kg (lighter to darker shade). (**E** to **H**) Acute treatment of lean male rats with a PEGylated GLP-1 mono-agonist and a PEGylated GLP-1/GIP co-agonist. Effects on (E and F) intraperitoneal glucose tolerance and plasma levels of (G) insulin and (H) C-peptide 10 min after a glucose challenge (n = 8). Plasma analysis was performed 24 hours after the subcutaneous injection of saline (black), a PEGylated GLP-1 mono-agonist (red), or a PEGylated GLP-1/GIP co-agonist (Table 1, compound 21, purple) at a dose of 10 nmol/kg. Data in (A) to (H) represent means ± SEM. *P < 0.05, **P < 0.01, ***P < 0.001, determined by ANOVA comparing vehicle to compound injections unless otherwise noted.

proper α/β cell ratio (fig. S7H), as well as glucagon and insulin immunoreactivity (fig. S7, I and J). Together, this improvement in islet cytoarchitecture is paralleled by an improvement in β cell functional capacity, as reflected by the homeostatic model assessment of fasted insulin to glucose, otherwise known as the HOMA-β score (fig. S7K). The collective rodent data illustrate two different GLP-1/GIP co-agonists that differ in duration of action, but each improves hyperglycemia and adiposity to a comparable level, which is to a greater extent than GLP-1 mono-agonists. Consequently, we have two different molecular candidates for exploring incretin co-agonism in nonhuman primates and humans.

Unimolecular dual incretins enhance insulinotropic effect in nonhuman primates

To determine whether the enhanced acute insulinotropic effect of the co-agonist observed in rodents translates to higher mammals, we administered a single injection of liraglutide or the acylated co-agonist (Table 1, compound 19) to cynomolgus monkeys. Blood glucose and plasma insulin were measured after an intravenous graded glucose infusion 24 hours after the peptide injection (Fig. 7A). Time-traced blood glucose levels during the challenge were decreased with liraglutide but were reduced to an even greater extent by the acylated co-agonist (Fig. 7B). Furthermore, a coordinated increase in plasma insulin (Fig. 7C) and C-peptide (Fig. 7D) was evident after treatment with liraglutide, and an even greater response was observed with the acylated co-agonist. Consistent with the enhanced efficacy in rodents, this acute exposure in nonhuman primates demonstrates the ability of a co-agonist to potentiate the insulin secretory response to a greater extent than liraglutide and warranted a similar investigation in human subjects.

Insulinotropic and antihyperglycemic effects of unimolecular dual incretins in humans

To determine whether a dual incretin co-agonist similarly enhanced the glucose-stimulated insulin secretory response in humans, we treated healthy nondiabetic subjects with escalating doses of the PEGylated co-agonist and measured glycemic control during a glucose infusion challenge in a comparable fashion to the study conducted in monkeys. Treatment with the PEGylated co-agonist (Table 1, compound 21) decreased blood glucose (Fig. 8A) and was paralleled by increases in plasma insulin (Fig. 8B). Collectively, these results demonstrate that the co-agonist can potentiate glucose-stimulated insulin secretion in humans and can effectively lower blood glucose excursions. Further investigation is required with a time action–matched GLP-1 agonist to determine whether the preclinically observed enhanced effect translates to human subjects.

Notably, in contrast to what is observed in humans with acute administration of the best-in-class GLP-1R agonists, treatment with the co-agonist was not associated with altered gut motility as assessed by measurement of acetaminophen absorption (Fig. 8C). At all three doses where enhancement of glycemic control was observed, there was no apparent effect on the levels of acetaminophen in plasma as opposed to the sizable effect observed with the shorter-acting GLP-1 agonist exendin-4, which is well recognized for its ability to induce unfavorable stasis of the gut. This lack of an effect on gastric motility coupled with a potent glycemic effect demonstrates that the two are not linked pharmacologically.

The initial safety, efficacy, and pharmacodynamics of the PEGylated co-agonist (Table 1, compound 21) were assessed in 53 patients with type 2 diabetes during a 6-week ascending-dose study. A dose-dependent increase in plasma concentration of the co-agonist was seen with treatment in the range of 4 to 30 mg. The median time to maximum observed concentration ranged from 68 to 120 hours, with a mean elimination half-life ranging from 120 to 141 hours after dose. The baseline HbA_{1c} levels ranged from 7.36 to 7.88%. There was a dose-dependent decrease in HbA_{1c} from baseline to day 43, which is 7 days after the sixth and final weekly dose of drug (Fig. 8D). The mean change from baseline for HbA_{1c} in patients who received active drug ranged from −0.53% for those receiving 4 mg to −1.11% for the cohort receiving 30 mg, compared to a decrease of 0.16% in the placebo cohort (Fig. 8D). Treatment up to 30 mg once weekly for 6 weeks was generally safe and well tolerated. All adverse events were considered to be mild or moderate in intensity. During the study, no patient experienced an adverse event of vomiting. Nausea was seen in 1 of 9 patients in the placebo group and in 2 of 12 in

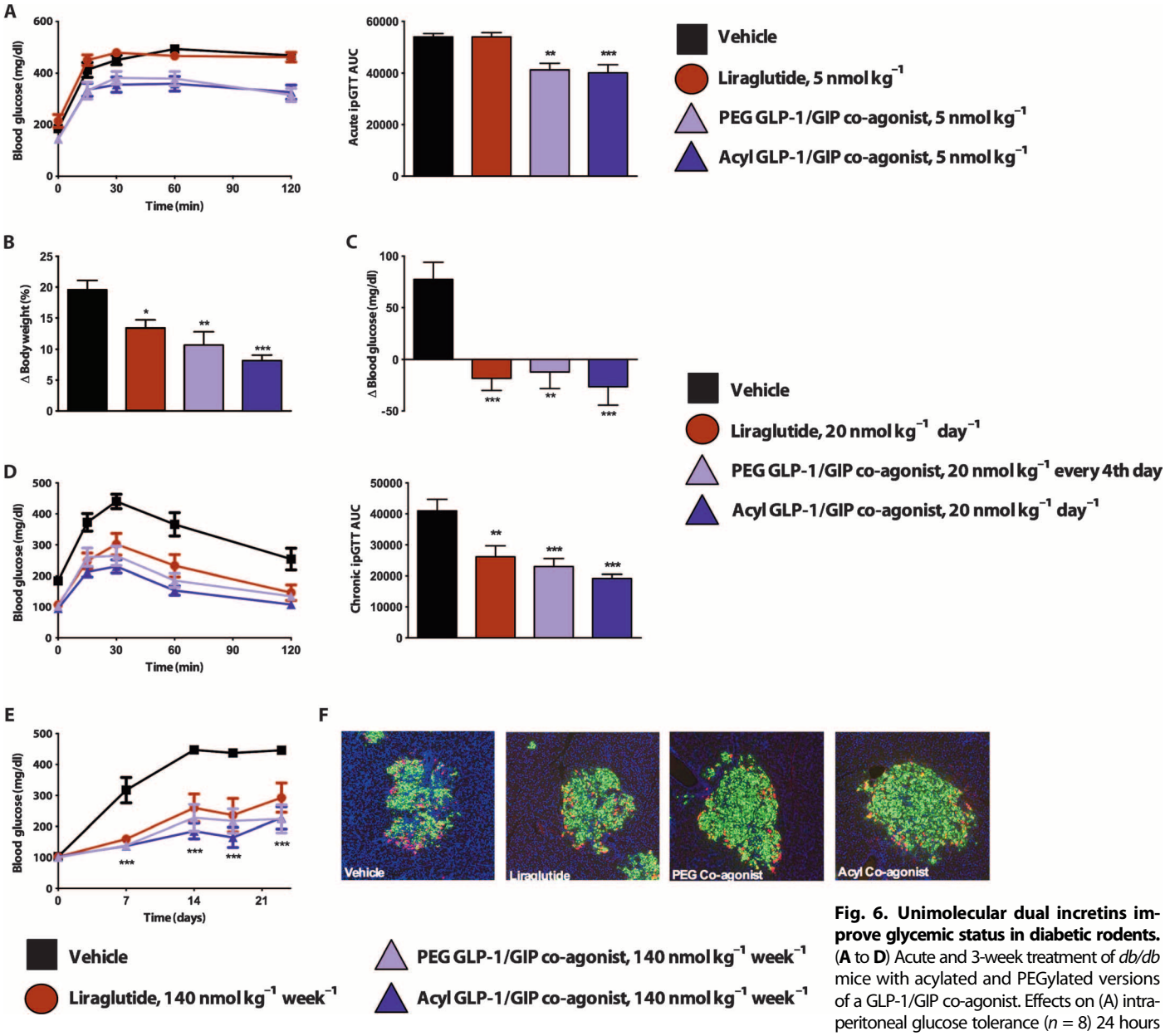

Fig. 6. Unimolecular dual incretins improve glycemic status in diabetic rodents. (**A** to **D**) Acute and 3-week treatment of *db/db* mice with acylated and PEGylated versions of a GLP-1/GIP co-agonist. Effects on (A) intraperitoneal glucose tolerance ($n = 8$) 24 hours after the subcutaneous injection of saline (black), liraglutide (red), a PEGylated GLP-1/GIP co-agonist (Table 1, compound 21, light purple/violet), and an acylated GLP-1/GIP co-agonist (Table 1, compound 19, dark purple/plum) at a dose of 5 nmol/kg. Effects on (B) body weight, (C) fasting blood glucose, and (D) intraperitoneal glucose tolerance ($n = 8$) after daily subcutaneous injections of saline (black), liraglutide (red), and an acylated GLP-1/GIP co-agonist (Table 1, compound 19, dark purple/plum) at a dose of 20 nmol/kg or after a subcutaneous injection every fourth day of a PEGylated GLP-1/GIP co-agonist (Table 1, compound 21, light purple/violet) at a dose of 20 nmol/kg (or 35 nmol/kg per week). (**E** and **F**) Three-week treatment of ZDF rats with acylated and PEGylated versions of a GLP-1/GIP co-agonist. Effects on (E) fasted blood glucose ($n = 8$) after daily subcutaneous injections of saline (black), liraglutide (red), and an acylated GLP-1/GIP co-agonist (Table 1, compound 19, dark purple/plum) at a dose of 20 nmol/kg or after a subcutaneous injection every fourth day of a PEGylated GLP-1/GIP co-agonist (Table 1, compound 21, light purple/violet) at a dose of 80 nmol/kg (or 140 nmol/kg per week). Effects on (F) islet morphology and immunohistochemistry for insulin (green), glucagon (red), and 4′,6-diamidino-2-phenylindole (DAPI) staining (blue). Data in (A) to (F) represent means ± SEM. $^{*}P < 0.05$, $^{**}P < 0.01$, $^{***}P < 0.001$, determined by ANOVA comparing vehicle to compound injections unless otherwise noted.

the 30-mg group, but not in any of the other dose groups. Diarrhea was seen in 2 of 12 in the 30-mg group. The rapid and sizable decreases in HbA_{1c} without vomiting and only minimal other gastrointestinal-related adverse effects suggest that the unimolecular dual incretins can be dosed even more aggressively to achieve superior outcomes.

DISCUSSION

Incretin mimetic therapy has exclusively been focused on the GLP-1 side of the incretin duality. Most of the approaches to optimize GLP-1 agonism for therapeutic purposes have focused on enhancing pharma-

cokinetics through chemical modifications and formulation strategies or exploring alternatives to delivery by injection (*24*). In contrast, our interest has focused on maximizing efficacy by integrating additional pharmacology to generate new unimolecular co-agonists (*25*, *26*). GLP-1–selective agonists provide sizable improvements in glycemic control, but only a fraction of patients achieve normalization, and most often, these selective agonists require combination with conventional oral agents (*27*). GLP-1 agonist therapy provides modest weight loss well below what is needed for sizeable metabolic improvements and often is accompanied by dose-limiting, adverse gastrointestinal events (*27*). Here,

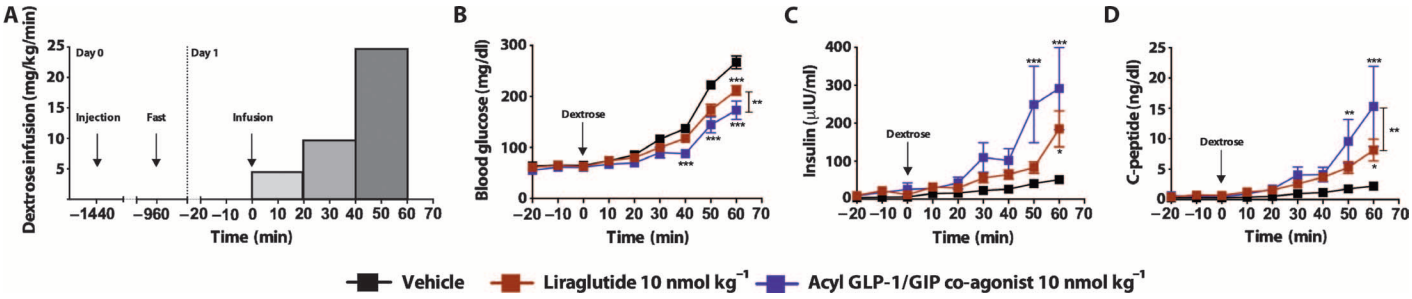

Fig. 7. A unimolecular dual incretin enhances insulinotropic response in monkeys. (**A** to **D**) Graded dextrose infusion in cynomolgus monkeys treated with an acylated GLP-1/GIP co-agonist. (A) Graded dextrose infusion schedule. Effects on (B) blood glucose, (C) plasma insulin, and (D) plasma C-peptide ($n = 4$) during an intravenous graded dextrose infusion in lean cynomolgus monkeys 24 hours after a single subcutaneous injection of saline (black), liraglutide (red), or an acylated GLP-1/GIP co-agonist (Table 1, compound 19, purple) at a dose of 10 nmol/kg. Data in (A) to (D) represent means ± SEM. $^{*}P < 0.05$, $^{**}P < 0.01$, $^{***}P < 0.001$, determined by ANOVA comparing vehicle to compound injections unless otherwise noted.

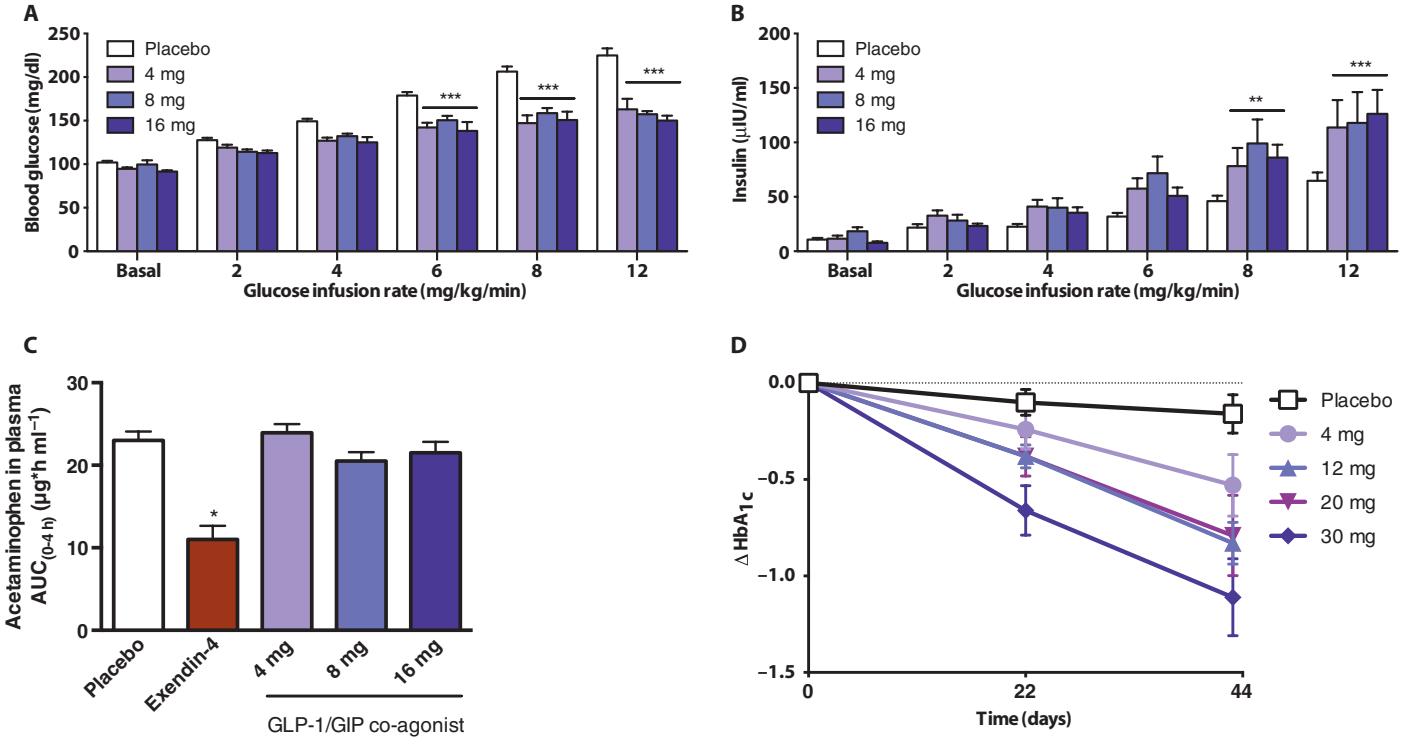

Fig. 8. A unimolecular dual incretin improves hyperglycemia in diabetic patients without gastrointestinal discomfort. (**A** to **C**) Graded dextrose infusion and safety assessment in healthy human subjects treated with a PEGylated GLP-1/GIP co-agonist. Effects on (A) blood glucose and (B) plasma insulin ($n = 6$) during a graded dextrose infusion in healthy human subjects 72 hours after a single subcutaneous injection of placebo saline (white) and escalating doses (total of 4, 8, and 16 mg) of a PEGylated GLP-1/GIP co-agonist (Table 1, compound 21, increasing shades of purple). Effect on the (C) plasma levels of orally administered acetaminophen (AUC from 0 to 4 hours) in subjects treated with a single subcutaneous injection of placebo (white), exendin-4 (red), or escalating doses of a PEGylated GLP-1/GIP co-agonist (Table 1, compound 21, purple). (**D**) Chronic treatment of type 2 diabetic patients with a PEGylated GLP-1/GIP co-agonist. Change in glycosylated HbA_{1c} (D) during 6 weeks of treatment with placebo (black) or escalating doses of the PEGylated GLP-1/GIP co-agonist (Table 1, compound 21, increasing shades of purple) in human patients with type 2 diabetes. Data in (A) to (D) represent means ± SEM. $^{**}P < 0.01$, $^{***}P < 0.001$, determined by ANOVA comparing placebo to compound injections unless otherwise noted.

we show that a balanced, unimolecular combination of GLP-1R and GIPR agonism provides greater metabolic efficacy than selective mono-agonism in different species from rodents to primates and humans, without apparent gastrointestinal discomfort.

Through a series of chemical changes that yielded a hybridized peptide sequence, a high-potency balanced agonist was identified. The co-agonist has native GLP-1 residues at positions 7, 13, 14, 17, 18, 19, 21, and 28 and GIP-specific residues at positions 1, 10, 12, 15, 16, 23, 24, and 27 (peptide 18, fig. S1). Examination of the sequence in more detail revealed that Ile^{12} was vital for selective GIP activity, whereas Ala^{18} was similarly important for GLP-1 activity. The first three residues and C-terminal amidation were found to be integral for selectivity at the GCGR. Substitution with Tyr^1, Aib^2, and Glu^3 not only substantially suppressed glucagon agonism but also served additional purposes—Tyr^1 increased GIP activity, Aib^2 protected against DPP-IV cleavage, and Glu^3 served as a key determinant residue conferring enhanced activity and selectivity at each incretin receptor. Activity at the two incretin receptors was also increased by Aib^{20} and the C-terminal extension. These modifications stabilized the helical secondary structure and provided a site for C-terminal chemical modifications to optimize pharmacokinetics. This balanced co-agonist was site-specifically modified by lipidation at Lys^{40} to generate an equally potent, longer-acting peptide suitable for once-a-day administration. PEGylation of the same peptide backbone with a 40-kD polymer at Cys^{24} lowered in vitro potency but yielded a highly effective, balanced therapeutic with time action suitable for once-a-week administration.

These dual incretin peptides increased insulin sensitivity and glycemic control in metabolically compromised rodent models of diet-induced obesity at a potency that was consistently enhanced 10-fold relative to comparably modified best-in-class selective GLP-1R agonists. A single acylated co-agonist proved more effective than liraglutide when comparatively tested in a graded glucose infusion assay in monkeys. In healthy human volunteers, the PEGylated analog demonstrated a similar ability to lower glucose in a dose-dependent fashion via an amplified insulin secretory response without any apparent gastrointestinal discomfort. Furthermore, the PEGylated co-agonist caused a dose-dependent decrease in HbA_{1c} levels over time in type 2 diabetic patients, with a maximal decrease of 1.11% from baseline at the highest dose tested (30 mg), demonstrating that the enhanced insulinotropic effect observed in healthy volunteers leads to a robust antidiabetic effect without adverse gastrointestinal side effects in type 2 diabetic patients. Collectively, the results indicate the potential for using GIP as an additional element to enhance the pharmacology of selective GLP-1R agonists by strengthening the inherent efficacy and broadening the therapeutic index. We believe that the combination of the enhanced efficacy and therapeutic index confers lower drug exposure as a consequence of lower constitutive receptor occupancy levels, thus closely resembling a physiological setting and circumventing the dose-limiting nausea complications that restrict current selective GLP-1R agonists. These clinical results support increases in dose to further enhance metabolic control and maximize weight loss, which can only be adequately assessed in longer-term studies. However, more in-depth toxicology analysis is warranted. In particular, a survey for altered capacity to induce formation of pancreatic lesions is justified by recent reports demonstrating an adverse role of GLP-1 pharmacology (*28*–*30*). Likewise, assessment of potential immunological responses derived from the foreign modifications introduced in the peptide, notably the Aib substitutions and PEG deposition in target cells, is equally warranted.

The recruitment of GIPR agonism for therapeutic purposes has been a controversial subject despite its well-recognized presence as an incretin partner to GLP-1. Although there is well-recognized alignment in GIP and GLP-1 pharmacology at pancreatic β cells (*31*), the basis for this skepticism is the belief that GIP pharmacology can promote obesity through lipogenic pathways (*5*–*11*, *32*–*35*). Concurrently, it has been observed that GIP glycemic action is lost to a greater degree than that of GLP-1 in metabolically compromised human subjects (*12*, *13*). Finally, preclinical observations with GIPR knockout rodents reported less weight gain on a high-fat diet challenge and an overall protection from glycemic disturbances (*6*, *7*), which was also observed with pharmacological GIP antagonism (*9*–*11*) and with transgenic ablation of GIP-producing intestinal K cells (*8*). However, recent evidence, including the pharmacology of the dual incretins presented here, indicates that the role of GIP in adipocyte biology is unclear.

The improved weight loss in response to adding GIP agonism to GLP-1 agonism, either in combination or with unimolecular co-agonism, is encouraging, although somewhat unexpected because of the aforementioned reports. We believe that our results are aligned with more recent reports of the beneficial metabolic benefits of GIP pharmacology, and that GIP demonstrates synergism with GLP-1 pharmacology, leading to an enhancement of these benefits. In particular, the progressive metabolic derangement in transgenic pigs that have a selective loss of pancreatic GIPR function occurs despite enhanced endogenous secretion of GLP-1 and despite a lack of fat mass accumulation (*15*), thus paralleling what is commonly observed in human disease. Likewise, mice treated with GIP analogs (*36*) or with transgenic GIP overexpression (*14*) are also protected from diet-induced obesity. Regarding a lack of inducible obesity in GIPR knockout rodents, similar observations were initially reported in GLP-1RKO rodents (*37*) despite the well-characterized weight-lowering pharmacology of GLP-1R agonists. This divergent response highlights the difficulties in using genetic loss-of-function models as predictors of pharmacological action and subsequent therapeutic success. Additionally, the purported GIP antagonist used to classify GIPR signaling as a target for attenuation in metabolic diseases has been characterized as a full yet weak agonist (*38*). We believe that there is a metabolic benefit in GIP pharmacology, and the previous concerns were incorrect. We observe that its supplementation with GLP-1 pharmacology leads to enhanced metabolic benefits in rodents that translate to acute glycemic benefits in primates. These collective results set the stage for clinical studies of extended duration where synergy with GLP-1 in reducing body weight can be explored. In such a setting, the improved glycemic control obtainable through GLP-1R agonism should restore GIP responsiveness and provide enhanced pharmacological benefit in a manner not possible through selective GIP agonism.

Through pharmacological and genetic loss-of-function models, we have demonstrated that each incretin constituent of the co-agonist is essential to achieve superior metabolic efficacy. We have yet to determine at a molecular level exactly how GLP-1 and GIP synergism results in an amplified metabolic response. Coordinated alterations in the physiology and hormonal sensitivities of metabolically active tissues may contribute to the negative energy balance; however, massive screening of metabolically relevant gene programs in liver, muscle, and adipose tissue did not reveal any unique insights to explain the beneficial interactions within the co-agonist. We speculate that the GLP-1 action can potentially alleviate the "brake" on GIP signaling that is evident within metabolic disease, thereby facilitating GIP to function at full metabolic capacity in concert with GLP-1. Herein, the coadministration of GLP-1 and GIP behaves similarly to GLP-1 mono-agonism through the first week of treatment, suggesting that GLP-1 pharmacology is

dominating the effect or that GIP pharmacology has limited efficacy, presumably due to a degree of resistance. However, after the first week, the GLP-1 effect begins to plateau, whereas the coadministration continues to drive weight loss. This body weight phenomenon is analogous to exendin-4 alone compared to coadministration with leptin (*16*), in which the weight loss driven by coadministration is enhanced only after leptin responsiveness is restored by adjunctive exendin-4 action.

Synergism at the cellular and molecular levels may be governing the amplified responses. We speculate that our unimolecular GIP/GLP-1 co-agonists could be inducing lateral interactions between the two constitutive receptors within the same cell, thus allosterically modulating the neighboring receptor's response to create a unique pharmacological outcome. Endogenous GLP-1 and GIP are reported to have opposing functions on receptor heterodimerization (*39*). Through actions mediated at the GIPR, cross-reactive GLP-1 binding promotes heterodimerization of the two receptors, whereas GIP antagonizes this response by displacing the bound GLP-1 to promote receptor dissociation (*39*). Much like the potential lipogenic effect of native GIP (*36*), it is suggested that these differences in dimer promotion between GLP-1 and GIP are derived from sequence differences within the C-terminal region (*39*). We speculate that the difference in the C-terminal sequence of the co-agonist compared to the native hormones, in combination with the high binding affinity at the GIPR, facilitates heterodimerization and maximizes in parallel the GLP-1 and GIP response. Together, this suggests that the cellular and molecular responses may be governed by the specific engineering of the dual incretins. The continued pursuit of a definitive molecular mechanism is a sizable, ongoing undertaking justified by the in vivo pharmacological experiments presented here.

Given that the co-agonist peptides have their origin in a glucagon-based sequence, we wondered whether residual glucagon agonism could be contributing to the metabolic efficacy despite confirmation of negligible in vitro glucagon activity. We concluded that glucagon agonism is not contributing to the in vivo pharmacology, because the dual incretin did not increase levels of circulating FGF21, an activity associated with the weight-lowering capacity of chronic glucagon agonism (*23*). Additionally, experiments in loss-of-function models for the GLP-1R and GIPR show that the co-agonist does not have the diabetogenic effects of acute glucagon, the weight-lowering effects of chronic glucagon pharmacology, or a glucagon-secretagogue action arising from GIP agonism (*19*, *40*). Furthermore, these results in loss-of-function models indicate that other off-target pharmacology outside of glucagon is not apparent in the co-agonist. Although we did not observe a glucagon-induced diabetogenic effect with the co-agonist in the GLP-1RKO mice, there was a powerful antihyperglycemic effect attributable to GIP agonism. Whether the response is exaggerated in these mice because of a compensatory mechanism arising from germ-line GLP-1RKO is uncertain. Although the exact functional and molecular underpinnings for metabolic benefits achieved by GLP-1/GIP synergism remain to be elucidated, the considerable metabolic benefits resulting from their combination are repeatable and certainly not the result of glucagon agonism.

In summary, we present a series of translational studies highlighting the optimization of molecular potency and time action preclinically to achieve substantial clinical efficacy without gastrointestinal discomfort. We demonstrate that unimolecular dual incretin co-agonists have enhanced insulinotropic activity to improve glycemic and body weight control in rodents. We demonstrate that this potentiated effect translates to nonhuman primates and functions with improved therapeutic index and efficacy in type 2 diabetic humans. The unique molecular pathway by which the metabolic improvements are derived is not known but is distinct from our previous report pertaining to glucagon agonism. These results highlight the strengths of this single-molecule combination therapy and broaden our perspective on how to achieve more effective treatments for chronic diseases. Together with the concept of single-molecule GLP-1R/GCGR co-agonism (*20*) and GLP-1/estrogen receptor co-agonism (*25*), the data presented here make it tempting to speculate that further advances in unimolecular poly-agonism might provide even greater potential for the treatment of metabolic diseases.

MATERIALS AND METHODS

Rationale and design of study

In vivo pharmacology studies were designed to assess the metabolic efficacy, most notably adiposity and glycemic endpoints, and safety of peptide analogs designed and confirmed to have co-agonistic properties at the GLP-1R and GIPR.

Randomization, replication, and outliers

In vitro receptor activation profiling of each analog was carried out in a minimum of three independent experiments. In vivo rodent pharmacology studies were performed in C57BL/6 mice, *db*/*db* mice, or ZDF rats in groups of six or more per treatment and were randomized before study initiation on the basis of body weight, body composition, and ad libitum–fed blood glucose. In vivo rodent pharmacology studies were validated in independent repeat follow-up studies. In vivo primate pharmacology studies were performed in cynomolgus monkeys in groups of four per treatment. Studies in healthy human subjects were placebo- and positive-controlled and single-blinded in male and female (non-childbearing potential) volunteers aged 18 to 55 years, which were preselected on the basis of a physical examination. The study in diabetic human subjects was placebo-controlled and performed in male and female volunteers aged 18 to 70 years with a diagnosis of type 2 diabetes for at least 3 months but no longer than 10 years. All data points were included in the analyses, and no outliers were excluded in calculations of means and statistical significance.

Peptide synthesis

Peptides were synthesized by solid-phase peptide synthesis methods using in situ neutralization for both butoxycarbonyl (Boc)– and 9-fluorenyl methoxycarbonyl (Fmoc)–based chemistries. For Boc-based neutralization peptide synthesis, 0.2 mmol of 4-methylbenzhydrylamine (MBHA) resin (Midwest Biotech) was used on a highly modified Applied Biosystems 430A peptide synthesizer by standard Boc methods using 3-(diethoxyphosphoryloxy)-(1–3)-benzotriazin-4 (3H)-one (DEPBT)/*N*,*N*-diisopropyl ethylamine (DIEA) for coupling and trifluoroacetic acid (TFA) for deprotection of N-terminal amines. Peptidyl resins were treated with hydrofluoric acid (HF)/*p*-cresol (10:0.5, v/v) at 0°C for 1 hour with agitation. HF was removed in vacuo, and the cleaved and deprotected peptide in diethyl ether was precipitated. For Fmoc-based neutralization peptide synthesis, 0.1 mmol of Rink MBHA resin (Novabiochem) was used on an Applied Biosystems 433A peptide synthesizer by standard Fmoc methods using diisopropylcarbodiimide (DIC)/6-chloro-1-hydroxybenzotriazole (Cl-HOBt) for coupling and 20% piperidine/dimethylformide for deprotection of N-terminal amines. Completed peptidyl resins were treated with TFA/triisopropylsilane (TIS)/anisole (9:0.5:0.5, v/v/v) for 2 hours with agitation. After removal of the ether, the crude peptide was dissolved in aqueous buffer containing at least

20% acetonitrile (ACN) and 1% acetic acid (AcOH) before lyophilization. Peptide molecular weights were confirmed by electrospray ionization (ESI) or matrix-assisted laser desorption/ionization time-of-flight (MALDI-TOF) mass spectrometry and character-confirmed by analytical reversed-phase high-performance liquid chromatography (HPLC) in 0.1% TFA with an ACN gradient on a Zorbax C8 column (0.46 × 5 cm).

Peptide purification

After cleavage from the resin, crude extracts were purified by semipreparative reversed-phase HPLC in 0.1% TFA with an ACN gradient on a Vydac C8 column (2.2 × 25 cm). Preparative fractions were analyzed for purity by analytical reversed-phase HPLC using the conditions listed above. Peptide molecular weights were confirmed by ESI or MALDI-TOF mass spectrometry. Purified peptides were lyophilized, aliquoted, and stored at 4°C.

PEGylation of peptides

Purified peptides were mixed at a 1:1 molar ratio with methoxy PEG maleimido-propionamide-40K (Chirotech) in 7 M urea and 50 mM tris (pH 8.0). Reaction progress was monitored by analytical reversed-phase HPLC, with free peptide being consumed within 1 hour. The reaction was quenched in 0.1% (v/v) TFA, purified, and characterized.

GLP-1R, GIPR, and GCGR activation

Each peptide was individually tested for its ability to activate the GLP-1R, GIPR, or GCGR through a cell-based luciferase reporter gene assay that indirectly measures cAMP induction. Human embryonic kidney (HEK) 293 cells were cotransfected with each individual receptor complementary DNA (cDNA) (zeocin selection) and a luciferase reporter gene construct fused to a cAMP response element (CRE) (hygromycin B selection). Cells were seeded at a density of 22,000 cells per well and serum-deprived for 16 hours in Dulbecco's modified Eagle's medium (HyClone) supplemented with 0.25% (v/v) bovine growth serum (HyClone). Serial dilutions of the peptides were added to 96-well cell culture–treated plates (BD Biosciences) containing the serum-deprived, cotransfected HEK293 cells, and incubated for 5 hours at 37°C and 5% CO_2 in a humidified environment. To stop the incubation, we added an equivalent volume of steadylite HTS luminescence substrate reagent (PerkinElmer) to the cells to induce lysis and expose the lysates to luciferin. The cells were agitated for 5 min and stored for 10 min in the dark. Luminescence was measured on a MicroBeta-1450 liquid scintillation counter (PerkinElmer). Luminescence data were graphed against concentration of peptide, and EC_{50} values were calculated with Origin software (OriginLab).

Animals

DIO mice and rats. C57BL/6 mice (Jackson Laboratories) were fed a diabetogenic diet (Research Diets), which is a high-sucrose diet with 58% kcal from fat. DIO mice were single- or group-housed on a 12:12-hour light-dark cycle at 22°C with free access to food and water. Mice were maintained under these conditions for a minimum of 16 weeks before initiation of pharmacological studies and were between the ages of 6 and 18 months. Wistar rats (Harlan) were fed a standard chow diet and single-housed on a 12:12-hour light-dark cycle at 22°C with free access to food and water. Rats for the acute studies were between the ages of 5 and 7 months.

GLP-1RKO mice. GLP-1RKO and wild-type littermates were bred in-house and fed the aforementioned diabetogenic diet.

db/db mice. Six-week-old male *db/db* mice (Jackson Laboratories) were housed four per cage and provided access to standard chow diet and water ad libitum. The mice were 9 weeks old when used for the indicated studies. The mice were randomized by ad libitum–fed blood glucose and body weight and were double-housed for the study.

ZDF rats. Seven-week-old male *ZDF* rats (Charles River Laboratories) were fed a special diet (Purina PMI 5008) and housed one per cage at room temperature (~21°C) and a relative humidity of 55 to 65%. A 12-hour light-dark cycle was maintained in the rooms, with all tests being performed during the light phase. Access to food and water was ad libitum. After 2 weeks of acclimatizing, measurement of fasting blood glucose levels for randomization was performed by tail puncture in conscious animals. ZDF rats were distributed into groups ($n = 8$ per group) according to body weight and fasting glucose levels.

All rodent studies were approved by and performed according to the guidelines of the Institutional Animal Care and Use Committee of the University of Cincinnati and F. Hoffmann–La Roche Ltd.

Rodent pharmacological and metabolism studies

Compounds were administered either by a single intraperitoneal injection for acute studies or via repeat subcutaneous injections at the indicated doses for chronic studies with the indicated durations. Body weights and food intake were measured every other day after the first injection. Fasted blood glucose was measured upon study initiation and termination after 6 hours of fasting.

Body composition measurements

Whole-body composition (fat and lean mass) was measured with nuclear magnetic resonance technology (EchoMRI).

Energy balance physiology measurements

Energy intake, energy expenditure, and home cage activity were assessed with a combined indirect calorimetry system (TSE Systems). O_2 consumption and CO_2 production were measured every 45 min for a total of 120 hours (including 12 hours of adaptation) to determine the respiratory quotient and energy expenditure. Food intake was determined continuously for 120 hours at the same time as the indirect calorimetry assessments by integration of scales into the sealed cage environment. Home cage locomotor activity was determined using a multidimensional infrared light beam system, with beams scanning the bottom and top levels of the cage, and activity being expressed as beam breaks.

Blood parameters

Blood was collected from tail veins after a 6-hour fast or after euthanasia, using EDTA-coated microvette tubes (Sarstedt), immediately chilled on ice, and centrifuged at 5000*g* and 4°C, and plasma was stored at −80°C. Plasma insulin and C-peptide were quantified by a radioimmunoassay from LINCO Research (Sensitive Rat Insulin RIA). Plasma FGF21 and leptin were quantified by enzyme-linked immunosorbent assays (Millipore and ALPCO, respectively). Plasma ketones, triglycerides, free fatty acids, cholesterol, ALT, and AST were measured by enzymatic assay kits (Thermo Electron). All assays were performed according to the manufacturers' instructions.

Glucose tolerance test

For the determination of glucose tolerance, DIO mice were subjected to 6 hours of fasting and injected intraperitoneally with glucose (2 g/kg) [20% (w/v) D-glucose (Sigma) in 0.9% (w/v) saline]. The *db/db* mice

were subjected to 6 hours of fasting and injected intraperitoneally with glucose (1 g/kg). Tail blood glucose levels were measured with a handheld glucometer (TheraSense FreeStyle) before (0 min) and at 15, 30, 60, 90, and 120 min after injection. For ZDF rats, oral glucose tolerance was assessed in six rats per group after an overnight fasting period (16 hours), and blood glucose was measured before oral glucose challenge (2 g/kg) and subsequently at 15, 30, 60, and 120 min after glucose challenge. Blood glucose was monitored with the Accu-Check glucometer system.

Histopathology and immunohistochemistry

The methodology has been described in detail elsewhere (*41*, *42*). In brief, tissue samples were fixed in 10% neutral-buffered formalin for 24 hours, dehydrated, and subsequently embedded into paraffin. The following immunofluorescence stainings on 4-μm tissue sections were carried out to assess islet morphology: anti-insulin (DAKO), anti-glucagon (R&D Systems), and DAPI (DAKO), followed by respective secondary fluorescent antibodies (Invitrogen). Digital imaging fluorescence microscopy of the pancreas was performed with a scanning platform (MetaSystems) with a Zeiss Imager Z.2 microscope (Carl Zeiss MicroImaging Inc.). Quantitative image analysis of islet morphology was performed with Definiens Architect XD (Definiens AG).

Graded dextrose infusion in cynomolgus monkeys

Twelve non-naïve male monkeys were selected from a colony, single-housed, maintained on a standard 12:12-hour light-dark cycle at 22°C with free access to a standard chow diet (Harlan) and water, and grouped according to matched body weights (5 kg) into three different treatment groups (n = 4). Twenty-four hours before the graded dextrose infusion, the monkeys were administered either saline or the peptides via a single subcutaneous injection. Monkeys from all test groups were fasted for 16 hours before initiation of the graded dextrose infusion. Thirty minutes before the dextrose infusion, the monkeys were sedated with Telazol (intramuscularly, 7 mg/kg), and an intravenous catheter for the dextrose infusion was placed in the cephalic vein. Baseline blood samples were obtained from the femoral artery or vein 20, 10, and 0 min before the infusion of dextrose. At 0 min, an infusion of a dextrose solution at 5 mg/kg per minute was initiated, and blood was collected after 10 and 20 min. Just after the 20-min blood sample was collected, the dextrose infusion rate was increased to 10 mg/kg per minute, and blood samples were again collected after 10 and 20 min of infusion at that rate (identified as 30 and 40 min). Just after the 40-min blood sample was collected, the dextrose infusion rate was increased to 25 mg/kg per minute, and blood was collected after 10 and 20 min of infusion at that rate (identified as 50 and 60 min). Blood was collected in EDTA- and aprotinin-containing (250 kallikrein inhibitory units/ml) tubes. Glucose, insulin, and C-peptide were measured in plasma, which was prepared from each of the blood samples described above. Plasma samples were provided to Millipore to measure compound concentration. Insulin was measured by a paramagnetic particle, chemiluminescent immunoassay (Beckman Coulter Access 2), and glucose was measured by the hexokinase method (Roche Hitachi 917). If necessary to complete the experiment, a booster anesthesia of ketamine (5 mg/kg) was administered.

All procedures in this protocol are in compliance with the U.S. Department of Agriculture's Animal Welfare Act (9 CFR Parts 1, 2, and 3); the *Guide for the Care and Use of Laboratory Animals*, Institute of Laboratory Animal Resources, National Academy Press, Washington, DC, 1996; and the National Institutes of Health, Office of Laboratory Animal Welfare. Whenever possible, procedures in this study are designed to avoid or minimize discomfort, distress, and pain to animals.

Graded dextrose infusion in human subjects

A randomized, placebo- and positive-controlled, sequential, two-part, single-blind study in healthy human volunteers was performed. The population for this study was males 18 to 55 years of age, inclusive, and females of non-childbearing potential 18 to 55 years of age, inclusive. Subjects were in good health on the basis of medical history, physical examination, 12-lead echocardiogram (ECG), and routine safety laboratory tests (blood chemistry, hematology, and urinalysis). Subjects had a body mass index of 20 to 30 kg/m^2, inclusive, were nonsmokers or had quit smoking >6 months before screening, and had negative alcohol and drug screens.

Part 1 served as the positive control for the study to determine whether effects on gastric emptying and insulin secretion rates were observed after treatment with exenatide. Part 2 of the study was designed to determine whether effects on gastric emptying and insulin secretion rates were observed after treatment with the GLP-1/GIP co-agonist. The study included a screening period of up to 21 days, a 3-day treatment period (part 1) or a 7-day treatment period (part 2), and one outpatient visit (part 2 only).

In part 1 of the study, after an overnight fast (≥10 hours), subjects (n = 6) received two subcutaneous injections of placebo (saline) on day 1 (2 hours apart, −120 and 0 min) in the abdomen. Body weight was measured at −120 min to calculate the graded glucose infusion, and baseline blood samples were drawn at −120, −15, and −10 min. At −10 min, subjects ingested a 1000-mg acetaminophen elixir with 240 ml of water. At 0 min, a graded glucose infusion (20% dextrose) was initiated, and the second subcutaneous injection of placebo was administered, and blood samples were drawn. Each level of the graded dextrose infusion lasted 30 min for a total of 2.5 hours and sequential rates of 2, 4, 6, 8, and 12 mg/kg per minute. Blood samples for measuring glucose, insulin, and C-peptide were subsequently drawn every 10 min for the duration of the infusion. Blood samples for acetaminophen concentration determination were drawn at −10, 30, 60, 90, 120, 150, 180, 240, 300, and 480 min, and an ECG was conducted at 210 min. On day 2 of part 1 of the study, the same protocol was followed, but instead of placebo injections, subjects received subcutaneous injections of exenatide (5 μg each, 2 hours apart) in the abdomen. On day 3, blood samples were drawn for safety tests, and an ECG was performed. In addition to the clinical laboratory safety assessments and ECGs, subjects were monitored for nausea events and severe hypoglycemia (≤70 mg/dl). All subjects were released from the investigational site on day 3, contacted via telephone on day 14 for a survey of adverse events, and subsequently discharged from the study.

Concurrently, a similar protocol was followed for part 2 of the study. However, instead of two subcutaneous injections, all subjects (n = 18) received a single subcutaneous injection of placebo (saline) in the abdomen 120 min before the dextrose infusion on day 1. The same graded dextrose infusion and blood drawing schedule was followed as outlined above. After an overnight fast, subjects (n = 6 per group) received a single subcutaneous injection of a GLP-1/GIP co-agonist in the abdomen on day 2, at a total dose of 4, 8, or 16 mg. Blood was drawn at 0 min for glucose, insulin, and C-peptide analysis. On day 5 (72 hours after dosing) and after an overnight fast, blood was drawn at −15 min before dextrose infusion for baseline plasma parameter analysis, and the same graded dextrose infusion was performed as outlined above. All subjects

in part 2 remained at the investigational site until day 7 with daily blood sample collection for safety tests. All subjects were released from the investigational site on day 7, contacted via telephone on day 14 for a survey of adverse events, subjected to an outpatient visit on day 28, and subsequently discharged from the study.

Initial assessment in type 2 diabetic patients

A randomized, placebo-controlled, ascending-dose chronic study to assess the safety, tolerability, pharmacokinetics, and pharmacodynamics of the PEGylated GLP-1/GIP co-agonist in type 2 diabetic patients was conducted. After a 2-week single-blind lead-in period, patients received either placebo or once-weekly subcutaneous injections of the PEGylated co-agonist for 6 weeks. Most of the studies were conducted on an outpatient basis except for the 4 days after the first and last dose of study drug. The first cohort of patients received 4 mg or matching placebo; the subsequent cohorts received 12, 20, and 30 mg or matching placebo. Each subsequent cohort was dosed after the safety of the previous cohort was assessed to be adequate. The population for this study was male and female patients 18 to 70 years of age, inclusive, with a diagnosis of type 2 diabetes ≥3 months and ≤10 years and treated with a stable dose of metformin. Patients were to have an HbA_{1c} of ≥6.5% and ≤10.5%, a fasting plasma glucose measurement of >110 and ≤240 mg/dl, and a body mass index of ≥25 and ≤42 kg/m^2. Patients were to be without acute or chronic medical conditions that would preclude participation in the study. Safety was assessed on the basis of adverse events, clinical laboratory assessments, physical examination, vital signs, and 12-lead ECGs. Blood samples were taken for HbA_{1c} at screening and at days 1, 22, and 43. Patients were instructed to obtain and record home capillary glucose values six times per week. Detailed pharmacokinetic assessments were done after the first and sixth dose of drug. A total of 53 patients were randomized to the study: 9 patients to placebo, 8 to 4 mg, 8 to 12 mg, 14 to 20 mg, and 14 to 30 mg. A total of 50 patients were in the primary safety and efficacy analyses. All data were analyzed with summary statistics.

Both of the above studies have been performed in accordance with International Conference on Harmonization E6 Guidance: "Good Clinical Practice: Consolidated Guidance" and applicable regulatory requirements at the Profil Institute for Clinical Research Inc. and Medpace Inc. Patients signed an informed consent form before any study procedures were performed. Patients were to meet all of the inclusion and none of the exclusion criteria to be eligible for the study participation.

Statistical analyses

Unless indicated otherwise, all statistical analyses were performed with GraphPad Prism. The analysis of the results obtained in the in vivo experiments was performed with one-way ANOVAs followed by Dunnett's tests. *P* values lower than 0.05 were considered significant. The results are presented as means ± SEM of six to eight replicates per group. Receptor activation data are presented as means ± SD.

SUPPLEMENTARY MATERIALS

www.sciencetranslationalmedicine.org/cgi/content/full/5/209/209ra151/DC1
Fig. S1. Sequences of native hormones and engineered analogs.
Fig. S2. Indirect calorimetry analysis in DIO mice.
Fig. S3. Pair-feeding comparison in DIO mice.
Fig. S4. Genomic profile of white adipose tissue, liver, and quadriceps.
Fig. S5. Comparison in GLP-1RKO mice.
Fig. S6. Effects on hepatic damage and steatosis in DIO mice.
Fig. S7. Effects on glycemia and islet cytoarchitecture in ZDF rats.

REFERENCES AND NOTES

1. J. G. Barrera, D. A. Sandoval, D. A. D'Alessio, R. J. Seeley, GLP-1 and energy balance: An integrated model of short-term and long-term control. *Nat. Rev. Endocrinol.* **7**, 507–516 (2011).
2. D. J. Drucker, The biology of incretin hormones. *Cell Metab.* **3**, 153–165 (2006).
3. A. Astrup, S. Rössner, L. Van Gaal, A. Rissanen, L. Niskanen, M. Al Hakim, J. Madsen, M. F. Rasmussen, M. E. Lean; NN8022-1807 Study Group, Effects of liraglutide in the treatment of obesity: A randomised, double-blind, placebo-controlled study. *Lancet* **374**, 1606–1616 (2009).
4. R. E. Amori, J. Lau, A. G. Pittas, Efficacy and safety of incretin therapy in type 2 diabetes: Systematic review and meta-analysis. *JAMA* **298**, 194–206 (2007).
5. S. J. Kim, C. Nian, C. H. McIntosh, Activation of lipoprotein lipase by glucose-dependent insulinotropic polypeptide in adipocytes. A role for a protein kinase B, LKB1, and AMP-activated protein kinase cascade. *J. Biol. Chem.* **282**, 8557–8567 (2007).
6. K. Miyawaki, Y. Yamada, H. Yano, H. Niwa, N. Ban, Y. Ihara, A. Kubota, S. Fujimoto, M. Kajikawa, A. Kuroe, K. Tsuda, H. Hashimoto, T. Yamashita, T. Jomori, F. Tashiro, J. Miyazaki, Y. Seino, Glucose intolerance caused by a defect in the entero-insular axis: A study in gastric inhibitory polypeptide receptor knockout mice. *Proc. Natl. Acad. Sci. U.S.A.* **96**, 14843–14847 (1999).
7. K. Miyawaki, Y. Yamada, N. Ban, Y. Ihara, K. Tsukiyama, H. Zhou, S. Fujimoto, A. Oku, K. Tsuda, S. Toyokuni, H. Hiai, W. Mizunoya, T. Fushiki, J. J. Holst, M. Makino, A. Tashita, Y. Kobara, Y. Tsubamoto, T. Jinnouchi, T. Jomori, Y. Seino, Inhibition of gastric inhibitory polypeptide signaling prevents obesity. *Nat. Med.* **8**, 738–742 (2002).
8. M. C. Althage, E. L. Ford, S. Wang, P. Tso, K. S. Polonsky, B. M. Wice, Targeted ablation of glucose-dependent insulinotropic polypeptide-producing cells in transgenic mice reduces obesity and insulin resistance induced by a high fat diet. *J. Biol. Chem.* **283**, 18365–18376 (2008).
9. V. A. Gault, F. P. O'Harte, P. Harriott, P. R. Flatt, Characterization of the cellular and metabolic effects of a novel enzyme-resistant antagonist of glucose-dependent insulinotropic polypeptide. *Biochem. Biophys. Res. Commun.* **290**, 1420–1426 (2002).
10. V. A. Gault, F. P. O'Harte, P. Harriott, M. H. Mooney, B. D. Green, P. R. Flatt, Effects of the novel (Pro^3)GIP antagonist and exendin(9–39)amide on GIP- and GLP-1-induced cyclic AMP generation, insulin secretion and postprandial insulin release in obese diabetic (*ob/ob*) mice: Evidence that GIP is the major physiological incretin. *Diabetologia* **46**, 222–230 (2003).
11. P. L. McClean, N. Irwin, R. S. Cassidy, J. J. Holst, V. A. Gault, P. R. Flatt, GIP receptor antagonism reverses obesity, insulin resistance, and associated metabolic disturbances induced in mice by prolonged consumption of high-fat diet. *Aml J. Physiol. Endocrinol. Metab.* **293**, E1746–E1755 (2007).
12. M. A. Nauck, M. M. Heimesaat, C. Orskov, J. J. Holst, R. Ebert, W. Creutzfeldt, Preserved incretin activity of glucagon-like peptide 1 [7-36 amide] but not of synthetic human gastric inhibitory polypeptide in patients with type-2 diabetes mellitus. *J. Clin. Invest.* **91**, 301–307 (1993).
13. T. Vilsbøll, F. K. Knop, T. Krarup, A. Johansen, S. Madsbad, S. Larsen, T. Hansen, O. Pedersen, J. J. Holst, The pathophysiology of diabetes involves a defective amplification of the late-phase insulin response to glucose by glucose-dependent insulinotropic polypeptide—Regardless of etiology and phenotype. *J. Clin. Endocrinol. Metab.* **88**, 4897–4903 (2003).
14. S. J. Kim, C. Nian, S. Karunakaran, S. M. Clee, C. M. Isales, C. H. McIntosh, GIP-overexpressing mice demonstrate reduced diet-induced obesity and steatosis, and improved glucose homeostasis. *PLoS One* **7**, e40156 (2012).
15. S. Renner, C. Fehlings, N. Herbach, A. Hofmann, D. C. von Waldthausen, B. Kessler, K. Ulrichs, I. Chodnevskaja, V. Moskalenko, W. Amselgruber, B. Göke, A. Pfeifer, R. Wanke, E. Wolf, Glucose intolerance and reduced proliferation of pancreatic β-cells in transgenic pigs with impaired glucose-dependent insulinotropic polypeptide function. *Diabetes* **59**, 1228–1238 (2010).
16. T. D. Müller, L. M. Sullivan, K. Habegger, C. X. Yi, D. Kabra, E. Grant, N. Ottaway, R. Krishna, J. Holland, J. Hembree, D. Perez-Tilve, P. T. Pfluger, M. J. DeGuzman, M. E. Siladi, V. S. Kraynov, D. W. Axelrod, R. DiMarchi, J. K. Pinkstaff, M. H. Tschöp, Restoration of leptin responsiveness in diet-induced obese mice using an optimized leptin analog in combination with exendin-4 or FGF21. *J. Pept. Sci.* **18**, 383–393 (2012).
17. N. M. Neary, C. J. Small, M. R. Druce, A. J. Park, S. M. Ellis, N. M. Semjonous, C. L. Dakin, K. Filipsson, F. Wang, A. S. Kent, G. S. Frost, M. A. Ghatei, S. R. Bloom, Peptide $YY_{3–36}$ and glucagon-like peptide-$1_{7–36}$ inhibit food intake additively. *Endocrinology* **146**, 5120–5127 (2005).
18. T. Talsania, Y. Anini, S. Siu, D. J. Drucker, P. L. Brubaker, Peripheral exendin-4 and peptide $YY^{3–36}$ synergistically reduce food intake through different mechanisms in mice. *Endocrinology* **146**, 3748–3756 (2005).
19. N. Mentis, I. Vardarli, L. D. Köthe, J. J. Holst, C. F. Deacon, M. Theodorakis, J. J. Meier, M. A. Nauck, GIP does not potentiate the antidiabetic effects of GLP-1 in hyperglycemic patients with type 2 diabetes. *Diabetes* **60**, 1270–1276 (2011).
20. J. W. Day, N. Ottaway, J. T. Patterson, V. Gelfanov, D. Smiley, J. Gidda, H. Findeisen, D. Bruemmer, D. J. Drucker, N. Chaudhary, J. Holland, J. Hembree, W. Abplanalp, E. Grant, J. Ruehl, H. Wilson, H. Kirchner, S. H. Lockie, S. Hofmann, S. C. Woods, R. Nogueiras, P. T. Pfluger, D. Perez-Tilve,

R. DiMarchi, M. H. Tschöp, A new glucagon and GLP-1 co-agonist eliminates obesity in rodents. *Nat. Chem. Biol.* **5**, 749–757 (2009).
21. J. Wu, P. Boström, L. M. Sparks, L. Ye, J. H. Choi, A. H. Giang, M. Khandekar, K. A. Virtanen, P. Nuutila, G. Schaart, K. Huang, H. Tu, W. D. van Marken Lichtenbelt, J. Hoeks, S. Enerbäck, P. Schrauwen, B. M. Spiegelman, Beige adipocytes are a distinct type of thermogenic fat cell in mouse and human. *Cell* **150**, 366–376 (2012).
22. T. Hansotia, L. L. Baggio, D. Delmeire, S. A. Hinke, Y. Yamada, K. Tsukiyama, Y. Seino, J. J. Holst, F. Schuit, D. J. Drucker, Double incretin receptor knockout (DIRKO) mice reveal an essential role for the enteroinsular axis in transducing the glucoregulatory actions of DPP-IV inhibitors. *Diabetes* **53**, 1326–1335 (2004).
23. K. M. Habegger, K. Stemmer, C. Cheng, T. D. Müller, K. M. Heppner, N. Ottaway, J. Holland, J. L. Hembree, D. Smiley, V. Gelfanov, R. Krishna, A. M. Arafat, A. Konkar, S. Belli, M. Kapps, S. C. Woods, S. M. Hofmann, D. D'Alessio, P. T. Pfluger, D. Perez-Tilve, R. J. Seeley, M. Konishi, N. Itoh, A. Kharitonenkov, J. Spranger, R. D. DiMarchi, M. H. Tschöp, Fibroblast growth factor 21 mediates specific glucagon actions. *Diabetes* **62**, 1453–1463 (2013).
24. D. Russell-Jones, S. Gough, Recent advances in incretin-based therapies. *Clin. Endocrinol.* **77**, 489–499 (2012).
25. B. Finan, B. Yang, N. Ottaway, K. Stemmer, T. D. Müller, C. X. Yi, K. Habegger, S. C. Schriever, C. García-Cáceres, D. G. Kabra, J. Hembree, J. Holland, C. Raver, R. J. Seeley, W. Hans, M. Irmler, J. Beckers, M. H. de Angelis, J. P. Tiano, F. Mauvais-Jarvis, D. Perez-Tilve, P. Pfluger, L. Zhang, V. Gelfanov, R. D. DiMarchi, M. H. Tschöp, Targeted estrogen delivery reverses the metabolic syndrome. *Nat. Med.* **18**, 1847–1856 (2012).
26. J. W. Day, P. Li, J. T. Patterson, J. Chabenne, M. D. Chabenne, V. M. Gelfanov, R. D. Dimarchi, Charge inversion at position 68 of the glucagon and glucagon-like peptide-1 receptors supports selectivity in hormone action. *J. Pept. Sci.* **17**, 218–225 (2011).
27. K. L. Edwards, M. Stapleton, J. Weis, B. K. Irons, An update in incretin-based therapy: A focus on glucagon-like peptide-1 receptor agonists. *Diabetes Technol. Ther.* **14**, 951–967 (2012).
28. B. Gier, A. V. Matveyenko, D. Kirakossian, D. Dawson, S. M. Dry, P. C. Butler, Chronic GLP-1 receptor activation by exendin-4 induces expansion of pancreatic duct glands in rats and accelerates formation of dysplastic lesions and chronic pancreatitis in the $Kras^{G12D}$ mouse model. *Diabetes* **61**, 1250–1262 (2012).
29. P. C. Butler, M. Elashoff, R. Elashoff, E. A. Gale, A critical analysis of the clinical use of incretin-based therapies: Are the GLP-1 therapies safe? *Diabetes Care* **36**, 2118–2125 (2013).
30. M. A. Nauck, O. Baranov, R. A. Ritzel, J. J. Meier, Do current incretin mimetics exploit the full therapeutic potential inherent in GLP-1 receptor stimulation? *Diabetologia* **56**, 1878–1883 (2013).
31. R. N. Kulkarni, GIP: No longer the neglected incretin twin? *Sci. Transl. Med.* **2**, 49ps47 (2010).
32. C. H. McIntosh, S. Widenmaier, S. J. Kim, Glucose-dependent insulinotropic polypeptide (gastric inhibitory polypeptide; GIP). *Vitam. Horm.* **80**, 409–471 (2009).
33. S. J. Kim, C. Nian, C. H. McIntosh, Resistin is a key mediator of glucose-dependent insulinotropic polypeptide (GIP) stimulation of lipoprotein lipase (LPL) activity in adipocytes. *J. Biol. Chem.* **282**, 34139–34147 (2007).
34. S. J. Kim, C. Nian, C. H. McIntosh, GIP increases human adipocyte LPL expression through CREB and TORC2-mediated trans-activation of the LPL gene. *J. Lipid Res.* **51**, 3145–3157 (2010).
35. T. Hansotia, A. Maida, G. Flock, Y. Yamada, K. Tsukiyama, Y. Seino, D. J. Drucker, Extrapancreatic incretin receptors modulate glucose homeostasis, body weight, and energy expenditure. *J. Clin. Invest.* **117**, 143–152 (2007).
36. S. B. Widenmaier, S. J. Kim, G. K. Yang, T. De Los Reyes, C. Nian, A. Asadi, Y. Seino, T. J. Kieffer, Y. N. Kwok, C. H. McIntosh, A GIP receptor agonist exhibits β-cell anti-apoptotic actions in rat models of diabetes resulting in improved β-cell function and glycemic control. *PLoS One* **5**, e9590 (2010).
37. L. A. Scrocchi, D. J. Drucker, Effects of aging and a high fat diet on body weight and glucose tolerance in glucagon-like peptide-1 $receptor^{-/-}$ mice. *Endocrinology* **139**, 3127–3132 (1998).
38. E. Faivre, A. Hamilton, C. Hölscher, Effects of acute and chronic administration of GIP analogues on cognition, synaptic plasticity and neurogenesis in mice. *Eur. J. Pharmacol.* **674**, 294–306 (2012).
39. D. Schelshorn, F. Joly, S. Mutel, C. Hampe, B. Breton, V. Mutel, R. Lütjens, Lateral allosterism in the glucagon receptor family: Glucagon-like peptide 1 induces G-protein-coupled receptor heteromer formation. *Mol. Pharmacol.* **81**, 309–318 (2012).
40. C. W. Chia, O. D. Carlson, W. Kim, Y. K. Shin, C. P. Charles, H. S. Kim, D. L. Melvin, J. M. Egan, Exogenous glucose-dependent insulinotropic polypeptide worsens post prandial hyperglycemia in type 2 diabetes. *Diabetes* **58**, 1342–1349 (2009).
41. A. Bénardeau, P. Verry, E. A. Atzpodien, J. M. Funk, M. Meyer, J. Mizrahi, M. Winter, M. B. Wright, S. Uhles, E. Sebokova, Effects of the dual PPAR-α/γ agonist aleglitazar on glycaemic control and organ protection in the Zucker diabetic fatty rat. *Diabetes Obes. Metab.* **15**, 164–174 (2013).
42. S. Uhles, H. Wang, A. Bénardeau, M. Prummer, M. Brecheisen, S. Sewing, L. Tobalina, D. Bosco, C. B. Wollheim, C. Migliorini, E. Sebokova, Taspoglutide, a novel human once-weekly GLP-1 analogue, protects pancreatic β-cells in vitro and preserves islet structure and function in the Zucker diabetic fatty rat in vivo. *Diabetes Obes. Metab.* **13**, 326–336 (2011).

Acknowledgments: We thank J. Levy for technical and chemical support of peptide synthesis; J. Ford for cell culture maintenance; J. Patterson, J. Day, B. Ward, and C. Ouyang for discussions on chemical structure–activity relationships; and C. Apfel for providing support with clinical chemistry measurements. **Funding:** Partial research funding was provided by Marcadia Biotech, which has been acquired by Roche Pharma, by the Helmholtz Alliance ICEMED (Imaging and Curing Environmental Metabolic Diseases) through the Initiative and Networking Fund of the Helmholtz Association, and by grants from the Deutsche Forschungsgesellschaft (TS226/1-1).
Author contributions: B.F. designed and performed in vitro, in vivo, and ex vivo rodent experiments; synthesized and characterized compounds; analyzed and interpreted the data; and wrote the manuscript. T.M. designed, synthesized, and characterized compounds; performed in vitro experiments; and analyzed and interpreted the data. N.O. designed and led in vivo pharmacology and metabolism rodent studies and interpreted the data. T.D.M., K. M. Habegger, K. M. Heppner, H.K., S.H.L., S.H., P.T.P., and D.P.-T. designed, supervised, and performed in vivo experiments and interpreted the data. J. Holland, J. Hembree, and C.R. performed in vivo pharmacology and metabolism studies in rodents. D.L.S. and B.Y. synthesized and characterized compounds and interpreted the data. V.G. designed and performed in vitro experiments and interpreted the data. D.B. performed ex vivo analysis and interpreted the data. D.J.D. gave advice on experimental design and interpreted the data. J.G., L.V., and L.Z. designed in vivo rodent, primate, and human experiments and interpreted the data. J.B.H. and M.L. designed and performed human clinical experiments and interpreted the data. M.B., S.U., W.R., E.H., E.S., K.C.-K., and A.K. designed and performed in vitro, in vivo, and ex vivo analyses and interpreted the data. R.D.D. and M.H.T. conceptualized, designed, and interpreted all studies and wrote the manuscript. **Competing interests:** R.D.D. is a cofounder of Marcadia Biotech and is currently a research consultant to Roche that supports ongoing scientific collaborations. D.J.D. has served as an advisor or consultant within the past 12 months to Arisaph Pharmaceuticals Inc., Diartis Pharmaceuticals, Eli Lilly Inc., Intarcia Therapeutics, Merck Research Laboratories, Novo Nordisk Inc., NPS Pharmaceuticals Inc., Receptos, Sanofi, Takeda, and Transition Pharmaceuticals Inc. Neither D.J.D. nor his family members hold stock directly or indirectly in any of these companies. R.D.D. and T.M. are co-inventors on patent applications (US2011/0166062 A1; US 12/999,285; "GIP-based mixed agonists for treatment of metabolic disorders and obesity") owned by Indiana University that pertain to the peptides in this paper that are licensed to Roche Pharmaceuticals (32993-214815). The other authors declare no competing interests.

Submitted 1 August 2013
Accepted 11 October 2013
Published 30 October 2013
10.1126/scitranslmed.3007218

Citation: B. Finan, T. Ma, N. Ottaway, T. D. Müller, K. M. Habegger, K. M. Heppner, H. Kirchner, J. Holland, J. Hembree, C. Raver, S. H. Lockie, D. L. Smiley, V. Gelfanov, B. Yang, S. Hofmann, D. Bruemmer, D. J. Drucker, P. T. Pfluger, D. Perez-Tilve, J. Gidda, L. Vignati, L. Zhang, J. B. Hauptman, M. Lau, M. Brecheisen, S. Uhles, W. Riboulet, E. Hainaut, E. Sebokova, K. Conde-Knape, A. Konkar, R. D. DiMarchi, M. H. Tschöp, Unimolecular dual incretins maximize metabolic benefits in rodents, monkeys, and humans. *Sci. Transl. Med.* **5**, 209ra151 (2013).

www.sciencetranslationalmedicine.org/cgi/content/full/5/209/209ra151/DC1

Supplementary Materials for

Unimolecular Dual Incretins Maximize Metabolic Benefits in Rodents, Monkeys, and Humans

Brian Finan, Tao Ma, Nickki Ottaway, Timo D. Müller, Kirk M. Habegger, Kristy M. Heppner, Henriette Kirchner, Jenna Holland, Jazzminn Hembree, Christine Raver, Sarah H. Lockie, David L. Smiley, Vasily Gelfanov, Bin Yang,Susanna Hofmann, Dennis Bruemmer, Daniel J. Drucker, Paul T. Pfluger, Diego Perez-Tilve, Jaswant Gidda, Louis Vignati, Lianshan Zhang, Jonathan B. Hauptman, Michele Lau, Mathieu Brecheisen, Sabine Uhles, William Riboulet, Emmanuelle Hainaut, Elena Sebokova, Karin Conde-Knape, Anish Konkar, Richard D. DiMarchi,* Matthias H. Tschöp*

*Corresponding author. E-mail: rdimarch@indiana.edu (R.D.D.); tschoep@helmholtzmuenchen.de (M.H.T.)

Published 30 October 2013, *Sci. Transl. Med.* **5**, 209ra151 (2013)
DOI: 10.1126/scitranslmed.3007218

The PDF file includes:

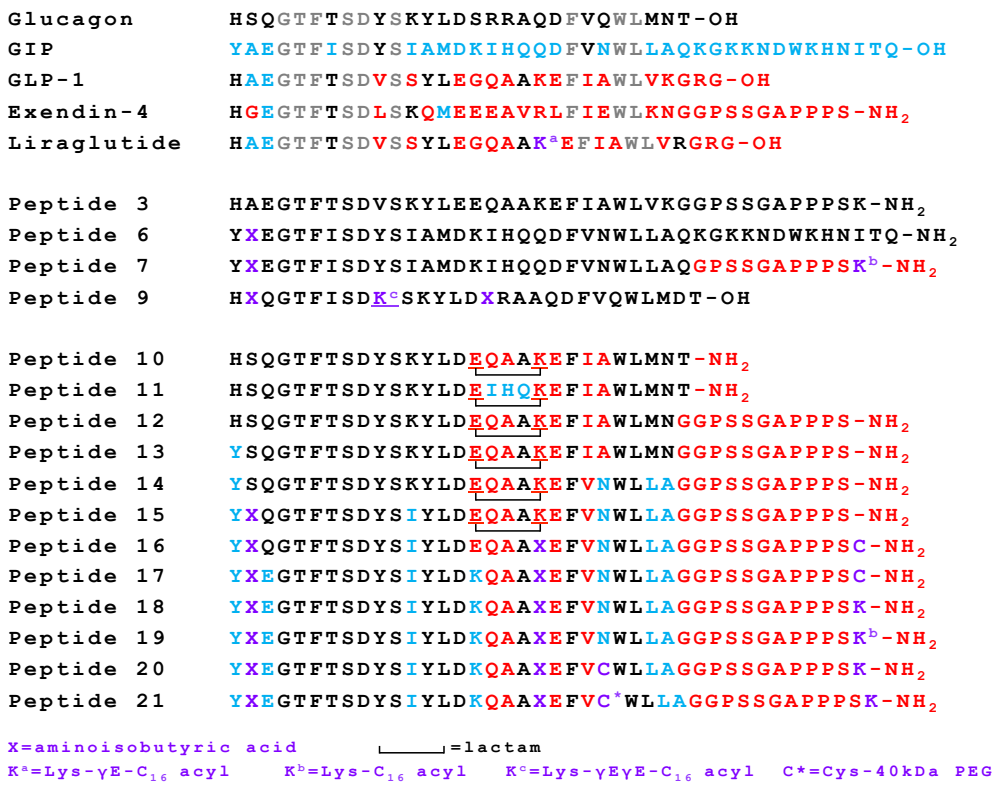

Supplemental Figure 1. Sequences of native hormones and engineered analogs. Sequence comparison of native glucagon, GIP, GLP-1, exendin-4, liraglutide and the engineered analogues leading to the GLP-1/GIP co-agonists (Table 1) with residues originating from glucagon highlighted in black, from GIP in blue, and from GLP-1 and/or exendin-4 in red. Foreign residues are highlighted in purple. Peptides 10-15 feature a 21-atom lactam macrocyclization between side chain residues of E^{16} and K^{20},and is highlighted by a bracket between these residues. Aminoisobutyric acid is denoted as X. Lysine with a γE-C_{16} acyl attached through the side chain amine is denoted as K^a. Lysine with a C_{16} acyl attached through the side chain amine is denoted as K^b. Lysine with a γEγE-C_{16} acyl attached through the side chain amine is denoted as K^c. Cysteine with a 40 kDa PEG attached through the side chain free sulfhydryl is denoted as C^*.

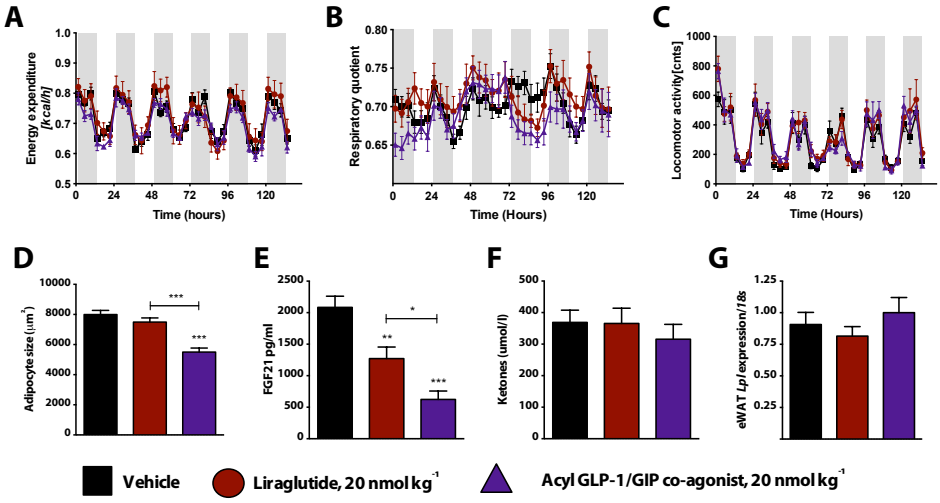

Supplemental Figure 2. Indirect calorimetry analysis in DIO mice. Four-week treatment of diet-induced obese male mice with bi-weekly doses of acylated versions of a GLP-1 mono-agonist and a GLP-1/GIP co-agonist. Effects on **(A)** energy expenditure, **(B)** locomotor activity, and **(C)** respiratory quotient (n = 8) during the last week of treatment. Effects on **(D)** epididymal white adipocytes, **(E)** plasma FGF21, **(F)** plasma ketones, and **(G)** relative expression of *lpl* in epididymal white adipose tissue (eWAT) from mice treated with vehicle (black), liraglutide (red), or an acyl GLP-1/GIP co-agonist (Table 1, compound 19, purple). Data in **(A–G)** represent means ± s.e.m. *P < 0.05, ** P < 0.01, *** P < 0.001, determined by ANOVA comparing vehicle to compound injections unless otherwise noted.

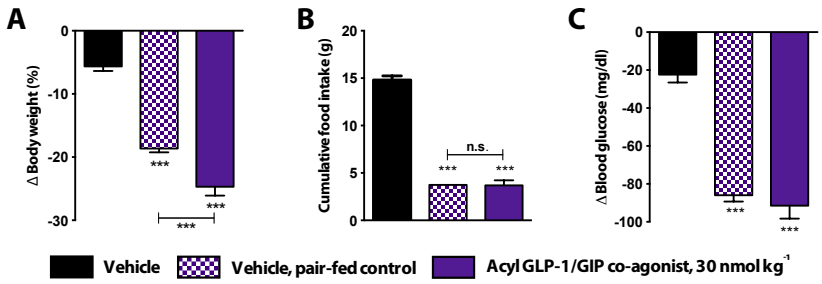

Supplemental Figure 3. Pair-feeding comparison in DIO mice. One-week treatment of diet-induced obese male mice with daily doses of an acylated GLP-1/GIP co-agonist compared to a pair-feeding control. Effects on **(A)** body weight, **(B)** food intake, and **(C)** *ad libitum* blood glucose (n = 8) following daily subcutaneous injections of saline (black), an acylated GLP-1/GIP co-agonist (Table 1, compound 19, purple) at a dose of 30 nmol/kg body weight compared to vehicle-treated mice that were pair-fed to co-agonist treated group (dotted purple). Data in **(A–C)** represent means ± s.e.m. *** $P < 0.001$, determined by ANOVA comparing vehicle to compound injections unless otherwise noted.

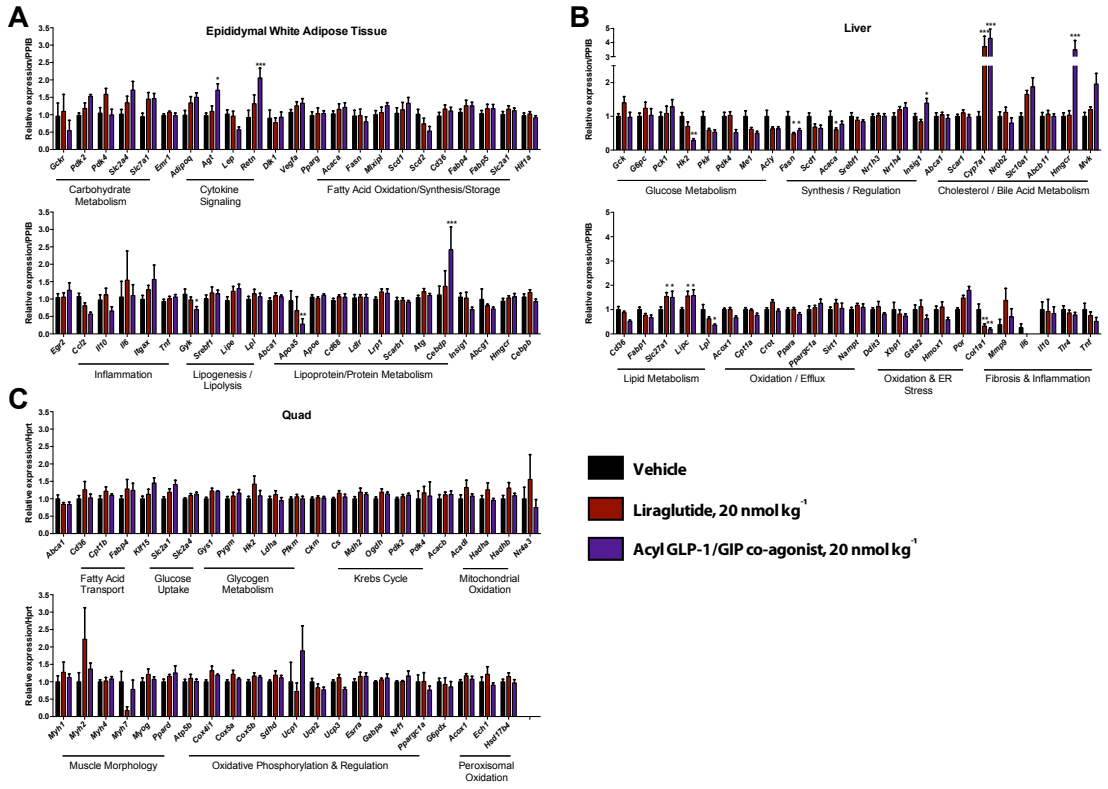

Supplemental Figure 4. Genomic profile of white adipose tissue, liver, and quadriceps. Four-week treatment of diet-induced obese male mice with bi-weekly doses of acylated versions of a GLP-1 mono-agonist and a GLP-1/GIP co-agonist. Effects on metabolically-relevant gene expression in **(A)** epididymal white adipose tissue, **(B)** liver, **(C)** and quadriceps (n = 8) following bi-weekly subcutaneous injections of saline (black), liraglutide (red), and an acylated GLP-1/GIP co-agonist (Table 1, compound 19, purple) at 20 nmol per kg body weight. Data in **(A–C)** represent means ± s.e.m. *$P < 0.05$, ** $P < 0.01$, *** $P < 0.001$, determined by ANOVA comparing vehicle to compound injections unless otherwise noted.

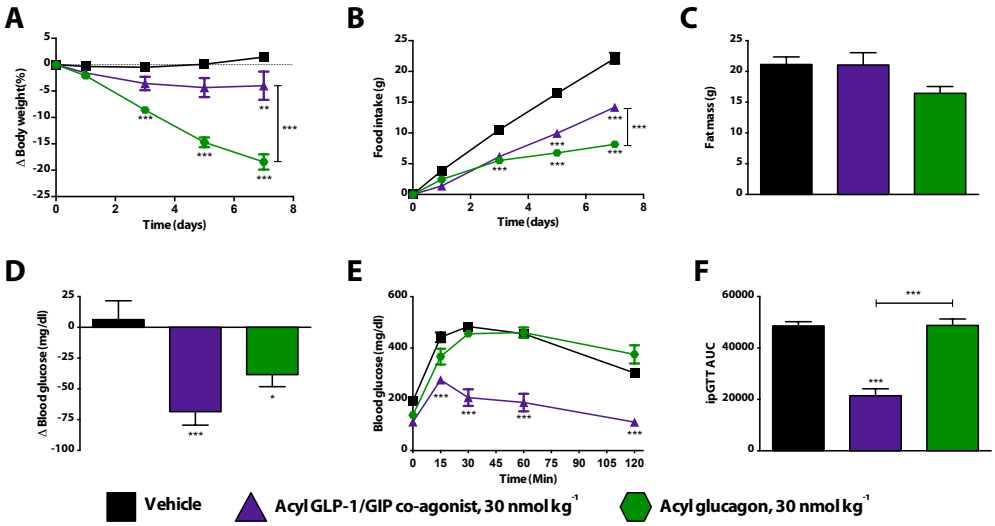

Supplemental Figure 5. Comparison in GLP-1RKO mice. One-week treatment of diet-induced obese GLP-1RKO male mice with daily doses of an acylated GLP-1/GIP co-agonist. Effects on **(A)** body weight, **(B)** food intake, and **(C)** fat mass, **(D)** fasted blood glucose, and **(E–F)** intraperitoneal glucose tolerance (n = 8) following daily subcutaneous injections of saline (black), an acylated GLP-1/GIP co-agonist (Table 1, compound 19, purple), or an acylated glucagon analogue (Table 1, compound 9[23], green) at a dose of 30 nmol/kg body weight. Data in **(A–F)** represent means ± s.e.m. *$P < 0.05$, ** $P < 0.01$, *** $P < 0.001$, determined by ANOVA comparing vehicle to compound injections unless otherwise noted.

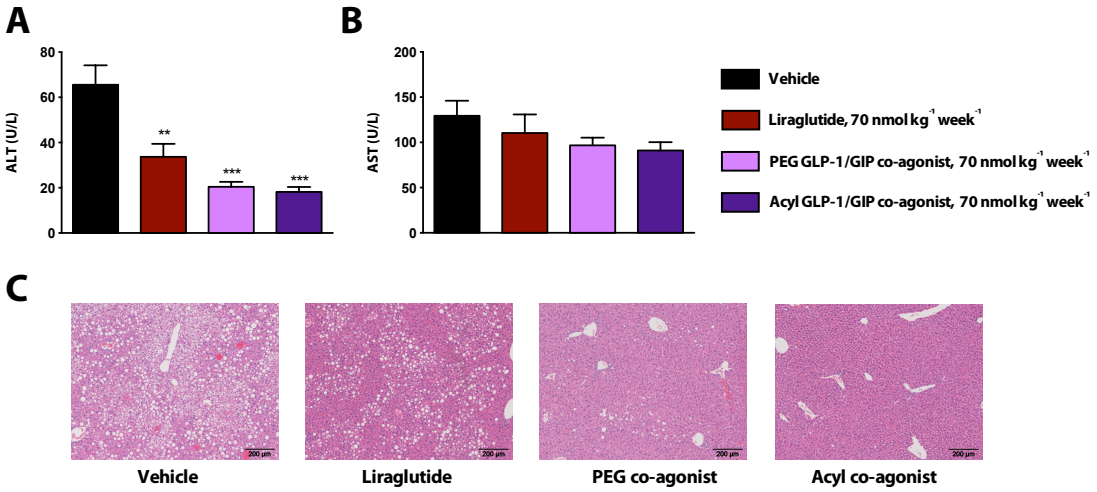

Supplemental Figure 6. Effects on hepatic damage and steatosis in DIO mice. Two-week treatment of diet-induced obese male mice with acylated and PEGylated versions of GLP-1/GIP co-agonists. Effects on **(A)** plasma ALT, **(B)** plasma AST, and **(C)** hepatic steatosis (n = 8) following daily subcutaneous injections of saline (black), liraglutide (red), and an acylated GLP-1/GIP co-agonist (Table 1, compound 19, dark purple); and weekly subcutaneous injections of a PEGylated GLP-1/GIP co-agonist at an equimolar weekly dose of 70 nmol per kg body weight (Table 1, compound 21, light purple/violet). Data in **(A–I)** represent means ± s.e.m. ** $P < 0.01$, *** $P < 0.001$, determined by ANOVA comparing vehicle to compound injections unless otherwise noted.

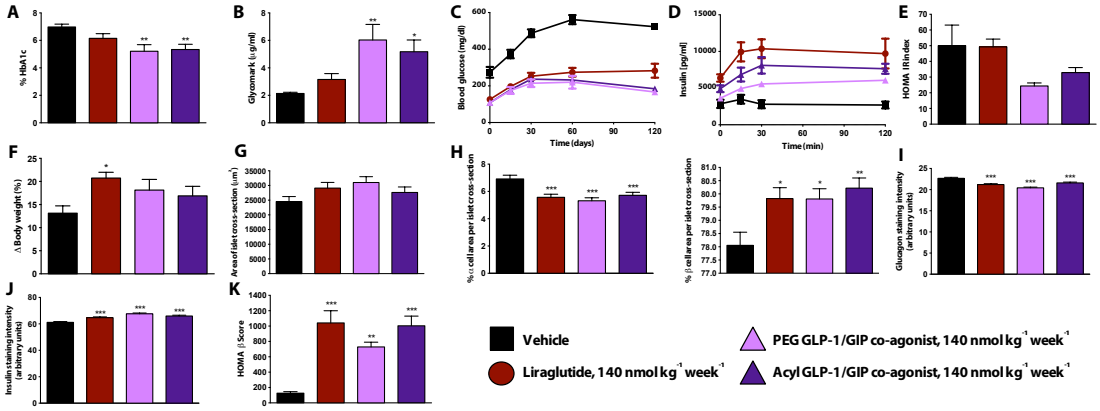

Supplemental Figure 7. Effects on glycemia and islet cytoarchitecture in ZDF rats. Glycemic and islet benefits following 3 weeks of treatment in ZDF rats. Effects on **(A)** HbA_{1C}, **(B)** glycomark, **(C)** intraperitoneal glucose tolerance, **(D)** insulin secretion during i.p. glucose challenge, **(E)** HOMA-IR score, **(F)** body weight, **(G)** area of islet cross-section, **(H)** percent α-cell and β-cell area per islet cross-section, **(I)** glucagon and **(J)** insulin staining intensity, and **(K)** HOMA-β score (n = 8) following daily subcutaneous injections of saline (black), liraglutide (red), and an acylated GLP-1/GIP co-agonist (Table 1, compound 19, dark purple/plum) at a dose of 20 nmol per kg body weight; or following a subcutaneous injection every fourth day of a PEGylated GLP-1/GIP co-agonist (Table 1, compound 21, light purple/violet) at a dose of 80 nmol per kg body weight (or 140 nmol per kg body weight per week) in ZDF rats. Data in **(A–K)** represent means ± s.e.m. *P < 0.05, ** P < 0.01, *** P < 0.001, determined by ANOVA comparing vehicle to compound injections unless otherwise noted.